A new MIS 3 radiocarbon chronology for Mochena Borago Rockshelter, SW Ethiopia: Implications for the interpretation of Late Pleistocene chronostratigraphy and human behavior

Steven Brandt [a,*], Elisabeth Hildebrand [b], Ralf Vogelsang [c], Jesse Wolfhagen [d], Hong Wang [e]

[a] Department of Anthropology, University of Florida, 1112 Turlington Hall, Gainesville, FL 32611, USA
[b] Department of Anthropology, Stony Brook University, Stony Brook, NY 11794-4364, USA
[c] Institute of Prehistoric Archaeology, University of Cologne, Bernhard-Feilchenfeld-Str. 11, 50969 Cologne, Germany
[d] Interdepartmental Doctoral Program in Anthropological Sciences, Stony Brook University, Stony Brook, NY 11794-4364, USA
[e] Illinois State Geological Survey, Prairie Research Institute, University of Illinois, Champaign, IL 61820, USA

ABSTRACT

With excavated layers spanning a period from >49 ka to ~36 ka, Mochena Borago Rockshelter reveals a complex sequence of Late Pleistocene human occupation punctuated by volcanic events. Fifty-nine radiocarbon ages make Mochena Borago one of the best-dated Late Pleistocene archaeological sites in eastern and northeastern Africa. However, complex site formation processes, dramatic stratigraphic differences between non-contiguous excavation areas, and "outlier" dates that appear in various parts of Mochena Borago's sequence, complicate efforts to develop a secure and detailed chronology for local and regional behavioral changes. This article focuses on contiguous squares within the Block Excavation Area (BXA) trench at the northern end of the shelter. Bayesian modeling of thirty-seven dates from six major lithostratigraphic units within the BXA yields a revised series of age ranges; these differ from the previous age model (derived from weighted means) in subtle but important ways. Perspectives gained through Bayesian analysis stimulate more careful consideration of the complex site formation processes operating at Mochena Borago, the contextual integrity of the site's robust and distinctive flaked stone artifact assemblages (lithics), and potential correlations between lithic changes and environmental events that occur on local, regional, and global scales. As these factors come into focus, Mochena Borago can serve as an important chronological benchmark to better understand human behavior in eastern and northeastern Africa around the time of the second major dispersal of *Homo sapiens*.

© 2016 Elsevier Ltd. All rights reserved.

1. Introduction

During Marine Isotope Stage (MIS) 4 (~74–57 ka) and MIS 3 (~57–29 ka) (Stewart and Jones, 2016) *Homo sapiens* successfully colonized most of the earth's continents. Initial dispersals of *H. sapiens* from Africa to southwest Asia ~125–100 ka took place during the warm, humid conditions of MIS 5. However, further dispersals apparently stalled as the cold and arid conditions of MIS 4 set in (Armitage et al., 2011; Drake et al., 2013; Hovers, 2006; Parton et al., 2013; Shea, 2008). Genetic and archaeological evidence points to new dispersals of *Homo sapiens* through and out of Africa during early MIS 3, with humans spreading east and north into southwest Asia and Mediterranean Europe, and south into temperate and tropical Asia and Australia by ~50–45 ka

(Armitage et al., 2011; Mellars, 2006; Mellars et al., 2013; Müller et al., 2011; Soares et al., 2011).

This rapid and unparalleled range expansion of our species has been one of the major questions driving Late Pleistocene archaeological and paleoanthropological research within these regions. Several scholars have hypothesized that toward the end of MIS 5, as conditions deteriorated into cold, hyper-arid MIS 4 in many parts of Africa, hunter-gatherer populations decreased and many groups were forced to migrate into environmental refugia (Brandt et al., 2012; Drake and Breeze, 2016; Stewart and Jones, 2016:8; Stewart and Stringer, 2012).

We propose it was in some of these MIS 4 refugia that various African innovations in technology, communication, mobility, and organization – which had developed during the late Middle Pleistocene in different places, at different times, and at different speeds by diverse hunter-gatherer groups (McBrearty and Brooks, 2000) – coalesced to form a novel blend of behavioral patterns. It was this distinct blend of "modern" cultural traits that permitted African hunter-gatherers to meet the challenges of their environmentally circumscribed MIS 4 world. During MIS 3, as African conditions ameliorated, albeit with

* Corresponding author.
E-mail addresses: sbrandt@ufl.edu (S. Brandt), elisabeth.hildebrand@stonybrook.edu (E. Hildebrand), R.Vogelsang@uni-koeln.de (R. Vogelsang), jesse.wolfhagen@stonybrook.edu (J. Wolfhagen), hongwang@illinois.edu (H. Wang).

frequent regional and local fluctuations (Jones et al., 2016), these same behaviors allowed human groups to not only move back and forth between Africa and Eurasia (Henn et al., 2012; Soares et al., 2016), but to achieve near-complete coverage of the world by the end of the Pleistocene (Klein, 2009).

One of the first steps in testing this hypothesis is to find securely dated Late Pleistocene sequences that span MIS 4 and/or MIS 3 in African refugia. Unfortunately very few such sites are known outside of South Africa (e.g., Haua Fteah in Libya (Douka et al., 2014) and Mumba in Tanzania (Diez-Martín et al., 2009)). Recent excavations at Mochena Borago Rockshelter in SW Ethiopia (Fig. 1) reveal that this site provides a secure, chronometrically dated paleoenvironmental and archaeological sequence for MIS 3, and possibly MIS 4, in a potential Late Pleistocene refugium within eastern Africa (Brandt et al., 2012).

The first published Late Pleistocene radiocarbon chronology for Mochena Borago drew upon 22 charcoal ^{14}C dates from the stratified deposits of the Block Excavation Area (BXA) at the northern end of the rockshelter (Fig. 2). Weighted means of ^{14}C dates from major strata produced a chronology spanning ~53–41 ka Cal BP (Brandt et al., 2012; Fisher, 2010). In this article, we use Bayesian modeling of 37 charcoal

ages to generate a revised chronology for the same Late Pleistocene stratigraphic units of the BXA. Our goals are to use the new Bayesian model to more precisely date Mochena Borago's Late Pleistocene lithostratigraphic sequence, gain a better temporal understanding of the site's complex formation processes, evaluate the contextual integrity and temporal patterning of its distinctive flaked stone artifact assemblages, and explore possible correlations between behavioral changes and environmental events at local, regional, and global scales. This should establish an important chronological benchmark for better understanding hunter-gatherer behavior in eastern and northeastern Africa during the time of the second major dispersal of *H. sapiens* through and out of the continent.

1.1. Current knowledge of chronometrically dated MIS 4 and MIS 3 archaeological sites near dispersal corridors: the Horn and northeastern Africa

Archaeological sites in the Horn of Africa (Djibouti, Eritrea, Ethiopia, Somalia/Somaliland) and northeastern Africa (Egypt, Sudan) are of particular interest because these regions are argued to be gateways for dispersals out of Africa via Northern and/or Southern Routes (Mellars,
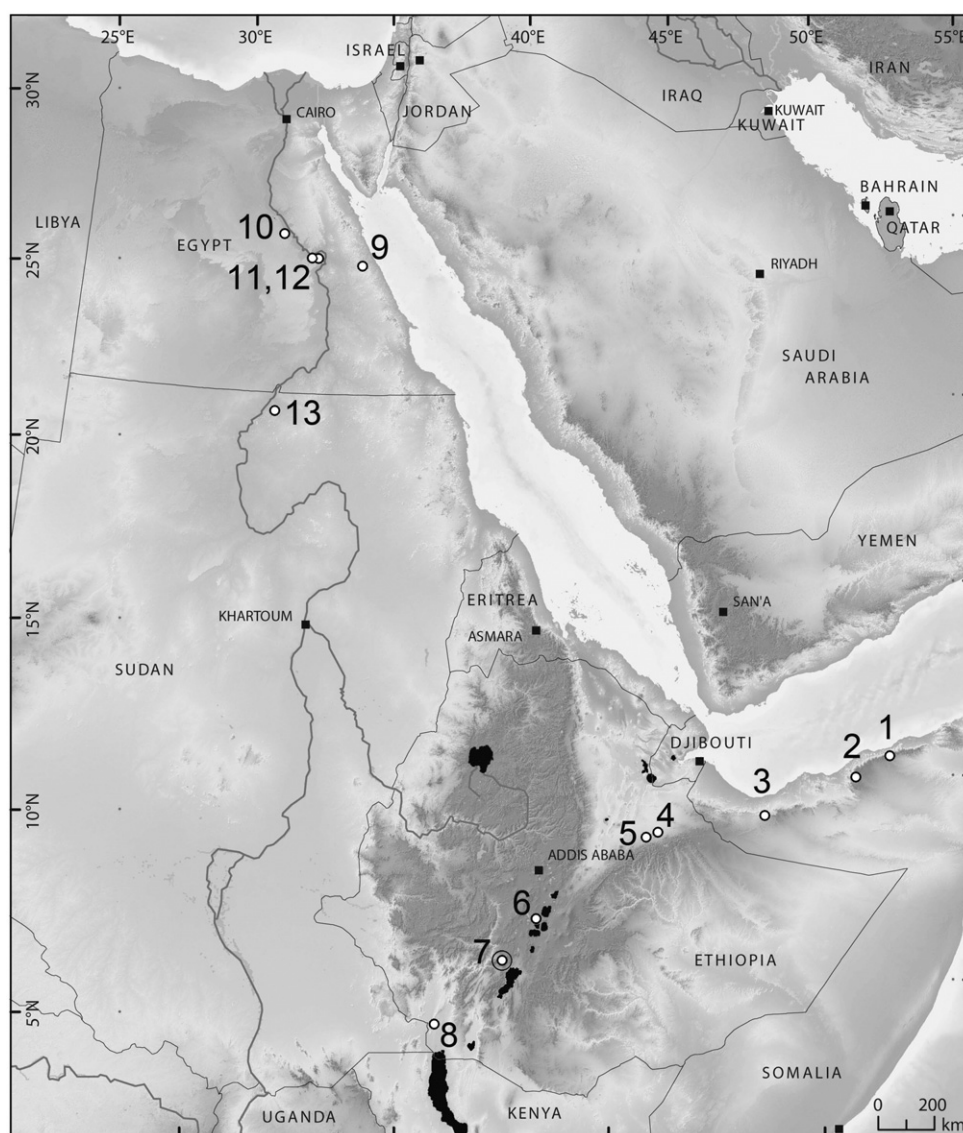

Fig. 1. Regional map with sites listed in text. 1 – Gud-Gud; 2 – Midhishi; 3 – Laas Geel; 4 – Porc Epic; 5 – Goda Buticha; 6 – Main Ethiopian Rift site area; 7 – Mochena Borago; 8 – Omo Kibish sites; 9 – Sodmein; 10 – Nazlet Khater (NK4); 11 – Nazlet Safaha; 12 – Taramsa 1; 13 – Khormusan Site 1017.
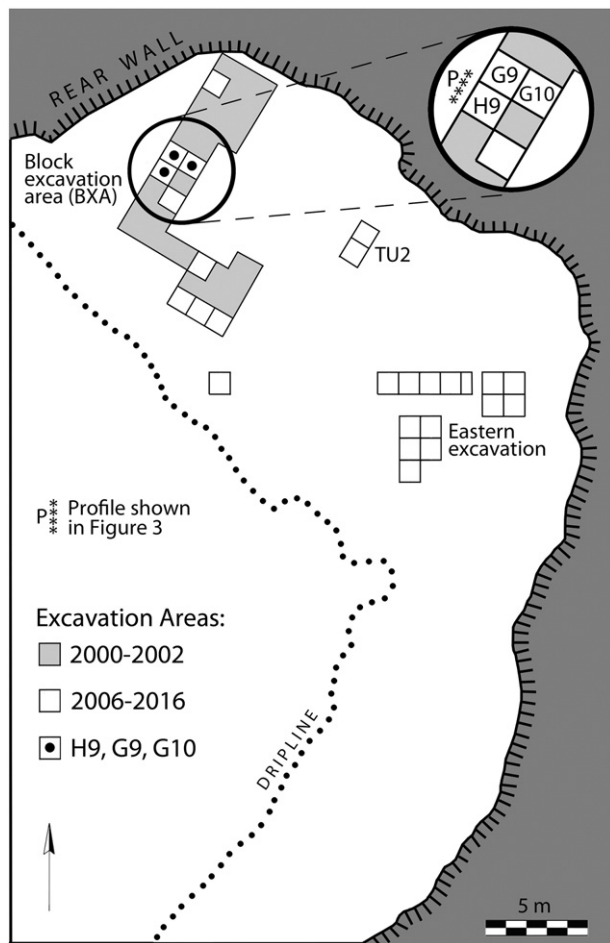
Fig. 2. Plan view of Mochena Borago Rockshelter.

2006) (Fig. 1). Unfortunately archaeological research in these regions has revealed very few sites with secure chronological sequences dating to MIS 4. Whether this reflects the difficulties of chronometrically dating sites in the ~70–60 ka range or represents a true abandonment of vast regions remains to be shown. Without securely dated and stratified sites from MIS 4, those from early MIS 3 merit especially close study because they provide evidence for continued occupation of refugia or re-occupation/colonization of regions by hunter-gatherers employing technologies established during MIS 4 and/or at the beginning of MIS 3. This section provides a summary of all known chronometric ages for sites in the Horn and northeast Africa that were occupied during MIS 4 and/or 3. It also briefly describes lithic assemblages as these artifacts form most if not all of the material remains at these sites.

Near the Southern dispersal route, securely dated evidence for human occupation of the Horn of Africa (Djibouti, Eritrea, Ethiopia, Somalia/Somaliland) during MIS 4-3 is scant and often problematic (Brandt, 1986; Brandt et al., 2012; Pleurdeau et al., 2014). Test excavations in 1982 at Midhishi 2 and Gud-Gud, two rockshelters in the highlands above the Gulf of Aden in northern Somalia/Somaliland, reveal artifact-bearing strata >40 ka in age. At Midhishi 2, Middle Stone Age (MSA) assemblages are associated with a single charcoal ^{14}C date of >40 ka, and include unifacial and bifacial points made on chert flakes struck from Levallois centripetal and point cores, including Nubian Type 1 forms (Brandt and Brook, 1984; Brandt and Gresham, 1989; Gresham, 1984). The test trench at Gud-Gud yielded a handful of lithics including an end scraper and blades associated with a single ^{14}C date on charcoal of >40 ka (Brandt, 1986). At the painted rockshelter of Laas

Geel 7 in northwest Somalia/Somaliland, recent excavations (Gutherz et al., 2014) have revealed lithic assemblages with mixed MSA and LSA (Later Stone Age) characteristics suggestive of J.D. Clark's Hargeisan Industry, but these are dated on the basis of only a single ostrich egg-shell (OES) ^{14}C sample to ~42 ka Cal BP.

Porc Epic Cave is situated on the southeastern edge of the Afar Rift in east-central Ethiopia, and overlooks a seasonal river basin near the city of Dire Dawa. Its MSA assemblages remain insecurely dated due to complex stratigraphy and several problematic dates: three contested obsidian hydration ages (61.2 ± 0.9, 61.6 ± 1, and 77.6 ± 1.6 ka), three ^{14}C ages on gastropod shell (33.7 ka, 35.6 ka, and >43.2 ka Cal BP), and a date of ~50 ka using low background gamma ray spectrometry on the early *Homo sapiens* mandible found in 1933 (Assefa, 2006; Clark and Williamson, 1984; Leplongeon, 2014; Pleurdeau, 2005; Rosso et al., 2014). Recent excavations at the nearby cave of Goda Buticha have uncovered lithic assemblages showing a mix of MSA and LSA attributes, and dated via four charcoal ^{14}C determinations to 46–33 ka Cal BP (Leplongeon, 2014; Pleurdeau et al., 2014). Recent fieldwork in the central part of the Main Ethiopian Rift has revealed a series of open-air and shelter sites containing blade-based LSA assemblages. As yet only one of these sites (DW1) dates to MIS 3 on the basis of a single ^{14}C charcoal age of ~33 ka Cal BP (Ménard et al., 2014).

Along the proposed Northern dispersal route in northeast Africa, only a handful of sites have chronometric ages, and even fewer are securely dated within the MIS 4-3 timespan. At Sodmein Cave in Egypt's Red Sea Hills, a deep stratified sequence spanning >100,000 years has four strata potentially dating to this interval (Mercier et al., 1999; Moeyersons et al., 2002; Schmidt et al., 2015; Van Peer et al., 1996; Van Peer and Vermeersch, 2000). The earliest is Layer G (MP4), dated by two charcoal ^{14}C samples to ≥30 ka and ≥45 ka. An OSL date of 89 ± 9 ka and a TL date of 87 ± 9 ka from a single sample within Stratum J, two layers deeper in Sodmein's sequence and below a major stratigraphic break, serve as a *terminus post quem* for Layer G. Classic Levallois and Nubian 1 lithic assemblages from these sites are assigned to the *Late Nubian Complex* of the 'Middle Paleolithic' (MP) (Van Peer 1996) now referred to as MSA (Van Peer, 2016; Wurz and Van Peer, 2012).

Sodmein Stratum F/G (MP3), which has a single ^{14}C age on charcoal (K. Kindermann pers. comm) of >45 ka, is also associated with MSA assemblages that include classic Levallois and Nubian Type 1 Levallois cores and debitage, as well as a few truncated-facetted pieces suggestive of connections to the Late Nubian Complex of the Nile Valley. Higher in the sequence, Layer F (MP2) has MSA assemblages dominated by a Levallois reduction strategy that includes a possible tanged Levallois flake. Although Van Peer et al. (1996) report two ^{14}C dates of ~29.95 ka and ≥30 ka (material and calibration unspecified) from this layer, Moeyersons et al. (2002:842) do not include these dates in their chronology. Layer E (MP1, undated but sandwiched between the dated strata F and D) has low densities of artifacts that include burins and two Emirah points. Finally, Layer D, which bears 'Upper Paleolithic' lithic assemblages emphasizing blades and single-platform cores, has only a single ^{14}C age of ~25.2 ± 5 ka (material and calibration unspecified) from an associated hearth (Van Peer et al., 1996).

Taramsa 1 is a late Pleistocene multi-activity chert quarry and burial site on a hill overlooking the west bank of the Nile in Upper Egypt (Fig. 1). In 1994 researchers discovered the poorly preserved, fragmentary remains of an anatomically modern child that had evidently been placed alongside the quarry extraction pits. One OSL date of 76.2 ± 4 ka from sand near the skull and another at 68.6 ± 8 ka from sediments overlying the burial represent the most likely age range for the associated late Nubian Complex lithics. Van Peer et al. (2010) argue that the youngest series of quarrying activities at the site are associated with the *Taramsan*, a transitional industry characterized by a distinct blade production strategy that developed out of a Levallois reduction system. The age of the Taramsan is problematic, but six OSL dates suggest 61.9 ± 7 to 56.9 ± 7 ka and possibly as late as ~40 ± 4 ka.

The *Lower Nile Valley Complex* (Van Peer and Vermeersch, 2000) is a distinct technological tradition characterized by classic Levallois assemblages thought to overlap temporally with the *Late Nubian Complex* referred to above. Chronometrically dated sites that best represent the Lower Nile Valley Complex include Nazlet Safaha 2 and Nazlet Khater 4 (Fig. 1). Nazlet Safaha 2, known for its distinctive Safaha reduction system, is OSL dated by a single sample to 59.8 ± 6.6 ka (Stokes and Bailey, 2002; Van Peer, 1991). Among several quarry sites on Nile terrace remnants overlooking the western Nile floodplain (Vermeersch, 2002), Nazlet Khater 4 is a localized set of ditches, vertical shafts, and galleries for extraction of cherts found in Nile gravel deposits (Leplongeon and Pleurdeau, 2011). Nine ^{14}C dates on charcoal from intact hearths, dumps in extraction shafts or ditches, and charcoal scatters range from ~35.1 ± 1.1 ka to 30.4 ± 2.3 ka (calibration unspecified) (Vermeersch et al., 2002). An OSL date yielded an age of 44.0 ± 6.0 ka (Stokes and Bailey, 2002).

The *Khormusan* industry is found at several sites overlooking the Nile near today's Egypt/Sudan border. There is little consensus on the timing of this industry, as chronometric dating of Khormusan sites has been problematic. Four charcoal radiocarbon ages obtained in the 1960s and 1970s yielded ages of 20.9 ± 0.28 ka, >36 ka, >36.7 ka and >41.4 ka; the 21 ka date is considered to be too young due to incomplete radiocarbon pretreatment, while the other three are minimal ages for the Khormusan that also reflect radiocarbon 'limits' for laboratories of that era (Wendorf et al., 1979). An unpublished U-Series date on ostrich eggshell indicates an age of 55 ± 5.6 ka (A. Marks pers. comm. 1992, cited by Sellet, 1995). However, Goder-Goldberger (2013) argues that OSL dates from geological localities in and around the Nile Valley suggest Khormusan sites may range from ~85–65 ka in age. Van Peer and Vermeersch (2000) included the Khormusan in the Nubian Complex, but Goder-Goldberger (2013) emphasizes affinities to eastern African MSA traditions, particularly between Khormusan Site 1017 and Omo Kibish sites BNS and KHS in southernmost Ethiopia, thereby implying that at least some of the Khormusan sites are of MIS 5 age.

This brief survey reveals the paucity of chronometrically dated evidence for human behavior during MIS 4 and MIS 3. Sites from the Horn have only ~eleven ^{14}C ages and three contested obsidian hydration dates, and sites from Sudan and Egypt have only ~eighteen ^{14}C ages, twelve OSL dates, and an unspecified number of U-series dates. Together, these regions span an area almost the size of the continental United States! Due to the current 50 ka "limit" on radiocarbon dating and calibration, as well as the inability to use OSL dating in volcano-derived sediments (Gliganic, 2011), it remains difficult to find sites with securely dated archaeological sequences from late MIS 4-early MIS 3 that can be used to gauge diachronic and synchronic changes in material culture during this critical period in the behavioral evolution of *Homo sapiens*. Mochena Borago Rockshelter in the highlands of southwest Ethiopia offers the opportunity to anchor one such sequence.

2. Mochena Borago Rockshelter

Positioned on the southwest side of Mt. Damota (Fig. 1), a dormant trachytic volcano overlooking the Main Ethiopian Rift northwest of Lake Abaya, Mochena Borago lies near the intersection of three major environmental systems within the Horn. To the west of Mt. Damota, the southwest Ethiopian highlands (>2700–500 m asl) contain habitats of Afromontane (highland), Transitional (midland), and Guinea-Congolian (lowland) forests cut by major river valleys. To the east and south, the Main Ethiopian Rift contains lakes and open vegetation in a dry, hot environment flanked by escarpments. Farther to the northeast, the Afar Depression is currently a vast lowland desert with scant rainfall and sparse vegetation. Hunter-gatherers would have had to be comfortable in this hostile environment in order to reach the Bab el Mandeb. The inhabitants of Mochena Borago would have been aware of most if not all of these environments, and may have made periodic use of any/all of them.

2.1. Context and history of research at Mochena Borago

Located in a ravine running down Damota's southwest flanks, Mochena Borago Rockshelter furnishes a large, open living space, with an opening almost 70 m wide, a height of 12 m, and a maximum distance of 20 m from dripline to rear wall. Its flat floor consists mainly of fine silt/clay surface material, punctuated by a few massive volcanic boulders in different areas. Today, the floor surface is dry, except where spray from the ravine's waterfall dampens sediment near the center of the dripline. During heavy rains, minor dripping from the roof of the shelter moistens the ground near excavation unit F9. However, local Wolaita remember significant water flow into the shelter from the northwestern side in recent times.

R. Joussaume led initial investigations at Mochena Borago in 1995, and in 1998 excavated a 1 × 1.5 m unit in the northern part of the shelter that revealed nearly 2 m of stratified archaeological deposits, including almost a meter of Late Pleistocene sediments (Gutherz, 2000). In 2000–2002 X. Gutherz, seeking evidence for early food production, directed excavations of Holocene deposits across >20 m² of the shelter's northern area, now known as the "Block Excavation Area" (BXA), as well as a test unit (TU2) a few meters to the east (Gutherz et al., 2002) (Fig. 2). Gutherz et al. later expanded excavations of Holocene deposits to the south.

In 2006 S. Brandt and E. Hildebrand established the Southwest Ethiopia Archaeological Project (SWEAP), and with E. Fisher excavated Mochena Borago's Late Pleistocene deposits from 2006 to 2008 with the aim of testing the hypothesis that southwest Ethiopia's highlands formed a refugium for human populations coping with the cold arid conditions of MIS 2, including the Last Glacial Maximum (LGM) (Brandt et al., 2012; Fisher, 2010). Excavations probed deeper within BXA units (G10, G9, H9, and I10) as well as units farther south (e.g., M13-15) (Fig. 2). SWEAP also opened a new series of excavation units aligned to cardinal directions in the eastern side of Mochena Borago, running west from N42E38. Nineteen charcoal dates yielded ages between 48 and 26 ^{14}C ka. With bedrock not yet reached, and no Late Pleistocene deposits postdating the onset of MIS 2, it became clear that although Mochena Borago might not shed light on human behavior during the LGM, it could offer important data for much of MIS 3 and perhaps even MIS 4.

From 2009–2014, research continued under the direction of S. Brandt (SWEAP) and R. Vogelsang (CRC 806, http://www.sfb806. uni-koeln.de) with the goal of documenting behavioral changes relevant to human dispersals out of Africa (Brandt et al., 2012). They continued to probe lower archaeological layers of BXA, including the lowest levels of units G9 and H9 just above a thick, impenetrable volcanic layer that forms the base of the BXA sequence (Fig. 3). Eighteen further AMS measurements focused on these occupation layers. Seeking evidence for MIS 4 occupation, the team also opened new trenches outside the BXA (Fig. 2) and found other complex stratigraphic sequences. Continued SWEAP excavations in 2015–2016 have opened and expanded new trenches in the eastern part of the shelter. Analyses relating these sequences to the BXA are ongoing, along with micromorphology sampling and geomorphological investigations of site formation processes. This paper only presents and analyzes radiocarbon dates from the Late Pleistocene BXA sequence.

2.2. Depositional history of Block Excavation Area (BXA)

Excavations in different parts of the rockshelter have revealed diverse, highly localized lithostratigraphic sequences. Because Bayesian analysis uses known stratigraphic relations to constrain phase models, it is best applied to contiguous deposits, such as BXA's major stratigraphic groups from PKT, the impenetrable basal volcanic layer, to BWT, an early Holocene tephra that caps the BXA Late Pleistocene sequence (Fig. 3). This descriptive overview of BXA's main strata draws upon previous stratigraphic information and depositional
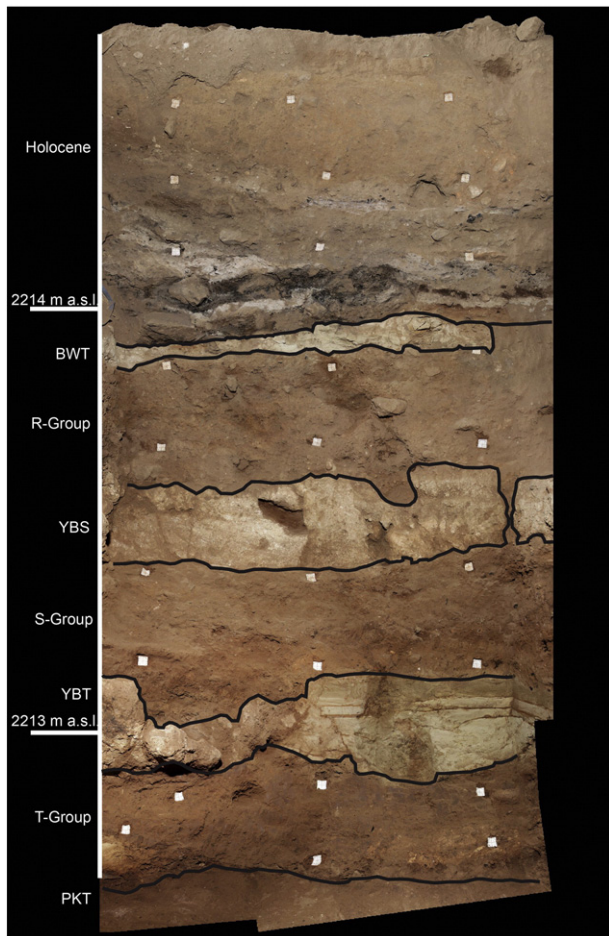
Fig. 3. Profile of NW wall of excavation unit H9 in the Block Excavation Area. Major stratigraphic groups are outlined.

interpretations prior to 2012 (Brandt et al., 2012; Fisher, 2010), as well as new data and observations obtained during the 2012–2015 field seasons (Meyer et al., n.d.).

The BXA lithostratigraphic sequence was formed by single to complex combinations of distinct processes. *Geogenic processes* include volcanic eruptions; stream incising, ponding, and other fluvial activities; shelter roof collapse or fall; wall collapse and erosion; chemical dissolution; and colluvial activities. *Anthropogenic processes* consist of human activities, such as the knapping, curating and discarding of flaked, ground and smoothed stone and ochre artifacts; the creation of combustion features and diffuse to dense concentrations of charcoal; and the discard of food remains exemplified by animal bones in various, but usually poor, states of preservation (Karkanas et al., 2015; Meyer et al., n.d.). Sediments formed through either or both processes may undergo subsequent *bioturbation* by plants (root growth), and by digging, tunneling and displacement by insects and other animals.

BXA's seven main strata (Fig. 3) are described from earliest (PKT, >49 ka) to latest (R-Group, ending ~39–36 ka). Dates for each major stratigraphic unit will be presented in Section 4.5 (Table 4), where readers can compare previously published weighted means (Brandt et al., 2012) with new age ranges derived from the Bayesian modeling undertaken in Section 4.

The volcanic layer PKT is the deepest and oldest stratum in the BXA sequence, and the only major BXA stratum that has yielded no datable material. Exclusively geogenic in origin (Meyer et al., n.d.), it is an extremely hard lahar (mud flow) that is especially difficult to penetrate in the small confines of 1 m² excavation units. At least 1 m thick and archaeologically sterile (Fisher, 2010), PKT is effectively the "bedrock" for

the BXA as we have been unable to reach any underlying deposits. However, it is not universal throughout the rockshelter as it appears to be missing in some of the other non-contiguous excavation units south and east of BXA.

The ~40 cm thick T-Group sediments (Fig. 3) unconformably overlie PKT and were formed by a mix of geogenic and anthropogenic processes, with some evidence for bioturbation even in recent times (e.g. tunneling by land crabs). They are divided into two sub-groups: 'Lower T-Group' and 'Upper T-Group' (Brandt et al., 2012; Fisher, 2010). Lower T-Group deposits have gravels, likely derived from the roof of the rockshelter, within a dark matrix that is indicative of high organic content. The heavily weathered, reworked clay coatings and calcite fillings suggest the periodic presence of small to large pools of standing water and/or slow moving streams during the more humid phases of early MIS 3. Upper T-Group sediments are redder and less weathered, suggesting stronger aeolian inputs and possibly drier conditions. However, compacted aggregates of fine, iron-rich illuvial clay bands also suggest periods of increased water flow. Both Lower and Upper T-Group facies provide clear evidence for human activities in the form of abundant flaked stone artifacts (lithics) and charcoal, as well as ochre, hematite, and poorly preserved, comminuted animal bone.

The geogenic YBT tephra consists of 20 cm of yellow-brown volcanic ash that overlies T-Group. Currently, we are uncertain if this contact is conformable or unconformable. The almost complete dearth of artifacts suggests a major interruption in human use of the shelter. In some areas, thin-bedded laminae suggest the tephra accumulated in small pools or slow-moving streams.

Formed by geogenic and anthropogenic processes, the ~30 cm thick S-Group sediments overlie YBT with a major unconformity (Fig. 3). S-Group deposits are characterized by a series of silty clays and dark brown silts with little gravel, and encompass large numbers of charcoal and lithics as well as ground/smoothed stone, worked pigments and poorly preserved bone indicative of renewed human activities. Some S-Group deposits show strong evidence for fluvial activity: a paleofluvial channel runs through G10, and many lithics show significant "damage" (Parow-Souchon et al., n.d.) that may be partly due to post-discard transport. Elsewhere, however, fluvial effects are not obvious, as sediment matrix is dominated by small particles (clays, silts).

YBS is a weakly sorted, consolidated yellow-brown silt that accumulated through colluvial action as a volcaniclastic mud flow with abundant ash and gravel (Brandt et al., 2012; Meyer et al., n.d.). It overlies the S-Group without any visible unconformity. At least 12 cm thick, it represents a second significant hiatus in human occupation as YBS has only a few lithics and pieces of charcoal, most of which appear to be in secondary context and emanating from overlying deposits.

Overlying YBS with only minor visible evidence for an unconformity, R-Group deposits are geogenic and anthropogenic in origin. About 30 cm thick on average, R-Group's matrix is clay/silt. Round to subrounded gravels are especially prevalent in Lower R-Group deposits and probably derive from roof-fall. The matrix has distinctive dark brown to reddish hues suggesting iron oxidation, and the porous microstructure in upper levels of R-Group has voids filled by oriented and laminated reddish orange clay particles (Fisher, 2010); micromorphology observations by P. Goldberg (pers. comm.) suggest standing water in parts of the BXA (Brandt et al., 2012). Abundant lithics and other materials indicate renewed human use of the rockshelter. More than two-thirds of the lithics show significant abrasion, ranging from angular to rounded, but around a third are fresh (Bermensolo, 2013). Together, R-Group deposits and lithics suggest discontinuous sedimentation in which artifacts were sometimes exposed on the surface for variable periods of time before they were subsequently covered in depositional events or displaced by erosion.

The BXA's Late Pleistocene sequence is capped by BWT, a dense, homogeneous white tephra derived from an early Holocene volcanic eruption (Fig. 3). The tephra entered Mochena Borago via aeolian processes,

settled in situ, and underwent minor rearrangement via fluvial processes in some areas, as the base of BWT is weathered and iron-stained. The R-Group/BWT interface shows only subtle signs of unconformity in the form of small concavities in R-Group's top surface. However, the long temporal gap (>20,000 years) between the two adjacent strata suggests major erosional processes must have come into play prior to the deposition of BWT.

2.3. Lithic technological changes in the MIS 3 levels of Block Excavation Area

The major artifact-bearing stratigraphic groups within BXA's late Pleistocene deposits have yielded >40,000 flaked stone (lithic) artifacts. Ground/smoothed stone and ochre artifacts also appear throughout the sequence. For now, we have refrained from establishing any kind of culture-stratigraphic framework, and instead for analytical purposes have used the Lower and Upper T-Groups, S-Group and R-Group natural lithostratigraphic units to place the assemblages within a chronological sequence (Table 1). Brandt et al. (2012) presented preliminary data from T-Group and S-Group assemblages; here we incorporate recent detailed analyses of R-Group lithics (Bermensolo, 2013; Parow-Souchon, 2013; Parow-Souchon et al., n.d.) and further examination of T-Group artifacts into a summary of technological trends within the BXA.

Perhaps the most distinguishing aspect of Mochena Borago's lithics is their diminutive size. The average length of lithics in each major stratigraphic group, and for every lithic type, is < 30 mm (Brandt et al., 2012; Ménard, 2015). This contrasts with most other sites in eastern Africa dating to the same general time period where artifacts tend to be significantly longer. Possible explanations for the small size of Mochena Borago's lithics include restricted access to raw materials, functional needs related to tools including weaponry (e.g. the bow and arrow), a "waste not want not" attitude toward core reduction, and "cultural tradition". We continue to explore these and other explanations through various avenues of research, including residue and use wear studies (V. Rots pers. comm.).

The overwhelming choice for lithic raw material was obsidian, forming at least 94% of all lithic assemblages (Table 1). Portable XRF analyses point to the eroded hills of Baantu on the western edge of the Rift ~20 km southeast of Mochena Borago as the source for most obsidian recovered at the rockshelter (Warren, 2010). This obsidian source is still used today by local crafters who make scrapers for working hides, a practice still in play among some ethnic groups in southwest Ethiopia (Brandt and Weedman, 2002). Stratified random surveys of Baantu identified multiple localities where large blocks quarried from flows, or weathered nodules collected on the surface were available in practically any size and shape. Surface scatters and the test excavation of an in-situ artifact concentration leave no doubt that obsidian knappers from the late Acheulian onwards worked at Baantu to reduce cores of varying types and sizes. This would make it difficult to argue that raw material constraints represent a viable explanation for small lithic size at Mochena Borago. A small percentage of Mochena Borago obsidian comes from source(s) other than Baantu, whose location(s) have yet to be identified.

One of the most puzzling aspects of the Mochena Borago lithic assemblages is the presence of abraded lithics in association with unabraded 'fresh' lithics. Rare in T-Group strata, they become common in S-Group and R-Group assemblages. We are examining various explanations for these "damaged" lithics, including chemical and fluvial processes as well as long periods of exposure on the surface of the shelter (Bermensolo, 2013; Parow-Souchon, 2013; Parow-Souchon et al., n.d.).

Mochena Borago knappers were clearly aware of a wide range of core reduction strategies, but chose to concentrate upon only one. The predominant core reduction strategy involves the production of elongated flakes and occasional blades from minimally prepared, tabular-shaped single, double, or multiplatform ("Tabular SDM") cores whose size and shape change little over time. Levallois reduction methods are surprisingly diverse given that they represent only 8–18% of all cores

Table 1

Representation of stone artifacts in assemblages analyzed so far from late Pleistocene excavations in Mochena Borago's Block Excavation Area (BXA).

Litho-strat group Category	Lower T N = 1059	Upper T N = 1953	S Group N = 3245	R Group *N = 1000
Raw material				
Obsidian	1000	1894	3239	981
Non-obsidian volcanics	31	55	1	9
Cryptocrystalline silicates	28	4	4	9
Quartzite	0	0	1	1
Total number	1059	1953	3245	1000
Extent of damage				
Fresh	1048	1914	2791	341
Damaged	11	39	454	659
Total number	1059	1953	3245	1000
Cores				
Tabular SDM	14	16	13	46
Levallois	3	2	1	5
Bipolar	0	0	7	6
Other/ irregular	0	0	1	5
Fragments	0	0	5	1
Total number	17	18	27	63
% total lithics	1.6%	0.9%	0.8%	6.3%
Debris				
Angular waste/shatter	4	50	142	119
Flakes blades	174	364	801	202
Flake/blade fragments	815	1398	2073	374
Levallois flakes	3	2	0	0
Levallois points	0	0	1	3
Core rejuvenation flakes	9	12	38	61
Burins spalls	1	0	6	7
Other/irregular	0	0	0	5
Total number	1006	1826	3061	771
% total lithics	95.0%	93.5%	94.3%	77.1%
Unshaped tools				
Nibbled ("utilized")	8	44	61	60
Modified	7	12	28	32
Flakes with bulbar thinning	0	0	0	1
Total number	15	56	89	93
% total lithics	1.4%	2.9%	2.7%	9.3%
Shaped Tools				
Backed	**0	11	24	15
Scrapers	7	11	30	18
Points	13	23	10	15
Burins	1	3	2	***23
Drills/awls/becs	0	2	2	1
Notches	0	1	0	1
Other/ irregular	0	2	0	3
Total number	21	53	68	76
% total lithics	2.0%	2.7%	2.1%	7.6%

* 50% random sample of lithics from preliminary analysis of unit G9 levels 3-13.

** Our most recent excavations have yielded backed pieces but these levels have not yet been fully analyzed.

*** Many are "technical" burins with only one flake scar.

from any stratigraphic group. They include small unidirectional and recurrent centripetal Levallois flake cores, classic unidirectional point cores, and remarkably small, thin Nubian Type 1 and 2 point cores. Other persistent but rare reduction strategies designed to produce flakes and irregular blades/bladelets include small discoidal and angular cores. Bipolar cores are rare in T-Group strata, but frequencies increase dramatically in S-Group and R-Group sediments. Small but classic prismatic/pyramidal and single- to multi-platform blade cores and their parallel-sided blades/bladelet products occur throughout the sequence, but in very small numbers (Parow-Souchon et al., n.d.).

As is the case with most eastern African Late Pleistocene assemblages, the importance of shaping (façonnage) is clearly reflected in the unifacial, parti-bifacial and bifacial points from Mochena Borago. In some instances, complex scar patterns attest to the considerable skill, time and effort knappers put in to the making of bifacial points, especially foliate and triangular-shaped ones. The points derive largely from small elongated flakes struck from Tabular SDM cores, although a few appear to be made from blades. Unretouched or minimally retouched classic Levallois and Nubian points are also present, but

rare. One of the few clear temporal changes in the Mochena Borago lith-ic sequence is diminishing frequency of points over time. Lower T-Group strata have the highest percentage of points throughout the se-quence, and also represent the highest frequency of shaped tools in that group (62%). Points drop to 42% of all shaped tools in Upper T-Group, and further still in S- and R-Groups.

Small backed pieces represent the other major temporal change in shaped tools. They are rare in the Lower T-Group, become more preva-lent in Upper T-Group, and continue to rise in frequency through the S-Group and R-Group assemblages, reaching the second highest percent-age of any shaped tool. All backed pieces but one (a crescent from Upper T-Group) are non-geometric in form. They are heterogeneous, and in-clude curved, straight and irregularly backed examples. Also present are backed flakes and blades/bladelets, some with use-wear on the op-posite edge, others with the backed edge and retouch on opposite edge forming an awl-like tip, and others with proximal or distal truncations. Other shaped tools include end and side scrapers, which consistently form ~20–40% of shaped tools from each Group, as well as a few drills, burins and notches.

2.4. Approaches to dating the Mochena Borago sequence

Our previous age model of Mochena Borago's Late Pleistocene se-quence relied on weighted means of twenty-two dates calibrated by CalPal 2007 (Weninger and Jöris, 2008) to generate probable age ranges for major stratigraphic groups (Brandt et al., 2012). The 2012 paper cal-culated weighted means via a Central Age Model (CAM), which has commonly been used for optically-stimulated luminescence (OSL) dat-ing in order to aggregate the log-paleodose results of multiple quartz grains in a sample, particularly when those results are over-dispersed from a common mean (Galbraith et al., 1999, 2005). Dates were weight-ed by the inverse of their standard deviation, which downplayed the contributions from dates with larger errors. As we built our initial age model (Brandt et al., 2012), weighted means struck us as a better way to generate age ranges for larger stratigraphic units rather than simply averaging dates within a stratum. However, reconsideration of the ap-plicability of the Central Age Model to radiocarbon dating has led us to re-evaluate our approach to dating BXA contexts.

Our initial premise that charcoal dates from the stratigraphic units at BXA can be considered a "population of samples that are assumed to have similar external influences" (Brandt et al., 2012:44) no longer ap-pears secure for cultural layers within the BXA. Each major stratigraphic group that is rich in artifacts (e.g., Upper T-Group) encompasses many depositional events – during which datable material entered the strati-graphic sequence multiple times from a variety of sources – rather than a single event whose timing we want to estimate (see Section 2.2). Thus, the charcoal samples found in Mochena Borago's Pleistocene cultural layers, and the many independent events they record, are poor analogs to multiple quartz grains within an OSL sample.

If multiple radiocarbon samples can be taken from a relatively dis-crete context (e.g., a hearth) that reflects a short-term single event anal-ogous to the dosing of quartz grains in OSL, then the Central Age Model might be appropriate to estimate a midpoint age of its use. The YBT and YBS tephra represent discrete events. However, because the charcoal found in these layers may not be directly associated with the volcanic events themselves (see Section 2.2), the Central Age Model is again inappropriate.

Mean dates for composite stratigraphic groups are therefore less useful for understanding depositional processes than an estimate of the start and end dates for each major stratigraphic group, which is pos-sible using Bayesian inference (Bayliss, 2009). The Bayesian analysis employed here models major stratigraphic units in a sequence. Each in-dividual unit is modeled as a uniform phase, meaning that we place no expected relationship on individual dates within each phase (Bronk Ramsey 2009a, b; see Section 4 for more details).

Switching to a Bayesian framework resolves four other disadvan-tages associated with use of weighted means. First, weighted means tend to be more heavily influenced by younger samples because older radiocarbon dates generally have larger standard deviations than youn-ger dates; this could skew the BXA chronology to be generally younger, and even allow intrusive dates from a later time period to have an exag-gerated influence on the sequence if their standard deviations are small. Bayesian analysis does not share this bias. Second, we saw that several dates were outliers with different possible causes, but lacked a mathe-matically rigorous way to assess outliers and prevent them from exercising undue influence on the weighted mean for a group. Methods for automatically identifying and rectifying outlier dates can be included in Bayesian models (Bronk Ramsey, 2009a, b). Third, the procedure of constructing weighted means did not make use of the fact that contigu-ous stratigraphy can help constrain date models (e.g., Lower T-Group deposits *must be* older than Upper T deposits). Bayesian modeling uses stratigraphic data to constrain the uncertainty of individual radio-carbon dates. Finally, because each weighted mean calculation generat-ed an age range that was represented as a normal distribution around a central point (e.g., 43,480 ± 443 cal BP for S-Group), weighted means could not generate probability distributions that were non-normal, bi-modal, or multimodal. Bayesian calibration directly draws from the IntCal 13 calibration curve, allowing date estimates to be expressed as probability ranges with multiple peaks (Buck et al., 1996:213).

3. Dating methods and results

Due to chronological proximity to the "dating barrier" (~40–50 ka), the MIS 3 deposits in Mochena Borago have presented challenges and opportunities for geochronological research. In 2007, we sought to com-pare results from multiple dating methods: radiocarbon dating of char-coal, OSL of rockshelter deposits, application of $^{40}Ar/^{39}Ar$ to tephra layers, and ESR of a tooth. Unfortunately, due to various properties of Mochena Borago and its sediments, only radiocarbon proved practicable (Brandt et al., 2012).

3.1. Radiocarbon sample collection, selection and curation

Following our first field season in 2006, we submitted six charcoal samples to the Illinois State Geological Survey (ISGS). To ensure suffi-cient charcoal for conventional ^{14}C dating, we combined charcoal finds from a single excavation unit and (maximum 5 cm) level into an aggre-gate dating sample. Thus each 2006 sample consisted either of all sieved charcoal pieces from a single square/level, or multiple plotted charcoal pieces from a single square/level. Collections included both sieved and plotted finds. All these samples all generated highly problematic results, likely due to mixing and/or contamination during sample collection, and are not presented here.

Beginning in 2007 and in all subsequent field seasons, we piece-plot-ted all artifacts, bone, and charcoal fragments >2 mm in size using Trim-ble TS-305 and Leica TS02 Total Stations. From 2007 on, all charcoal samples were submitted for AMS dating. Each sample represented an individual occurrence of charcoal within a 1 cm^3 area. Most samples were much smaller than 1 cm^3 – more typically 2–5 mm in any dimen-sion. In most cases charcoal was tightly gripped by surrounding matrix, usually a compacted silt/clay. These conditions seemed ideal for preventing vertical or horizontal slippage, but also caused fragmenta-tion during recovery. Small size and breakage together impeded identi-fication of the type of carbonized plant tissue (e.g., wood, stem, leaf, or fruit). In some cases, the charred material appeared to be a structurally intact chunk of carbonized plant material, but in others, it was not clear whether tissues were still in their original form.

To avoid contamination during collection, and due to the fragile state of the samples, we did not attempt to separate charcoal from its sur-rounding matrix. All radiocarbon samples were collected and handled using metal spoons or tweezers, and placed directly into a plastic bag.

(Aluminum foil was not used because it contains lubrication oil that may contaminate samples.) All dates presented here reflect this protocol: they are from individually piece-plotted, untouched charcoal samples. Twenty-four samples were submitted to the Illinois State Geological Survey's Radiocarbon Dating Laboratory (ISGS) between 2007 and 2014, and thirteen were submitted to the University of Cologne Centre for Accelerator Mass Spectrometry (COL) between 2012 and 2014.

3.2. Sample treatment and processing

We considered the relative merits of Acid-Base-Acid (ABA), Acid-Base-Oxidation (ABOx) and high temperature pyrolysis pretreatments. Various concerns shaped our choice of pretreatment methods. ABA pretreatments have a long history of use and are well known (Brock et al., 2010). ABOx pretreatments use a solution of potassium dichromate and sulphuric acid ($K_2Cr_2O_7 + H_2SO_4$) to further oxidize acid-base pretreated charcoal samples (Bird et al., 1999). Some studies have shown that ABOx can improve age determination of charcoal samples up to 55 ka by more thorough removal of younger carbon contaminants (Bird et al., 1999; Higham et al., 2009; Santos et al., 2003; Turney et al., 2001). In split-sample comparison tests of ABOx vs. ABA, the ABOx method has indeed generated older dates than the ABA method in some cases; however, in other cases ABOx yielded similar or younger ages than ABA (Haesaerts et al., 2013; Rebollo et al., 2011).

ABOx pretreatment also raises two concerns. First, use of H_2SO_4 in the wet oxidation stage releases volatile sulphur compounds that hinder the graphitization step just prior to AMS ^{14}C measurements, potentially decreasing sample size and thus increasing dating uncertainties (Santos et al., 2003). Second, the solution of potassium dichromate and sulphuric acid is a strong oxidation agent that severely degrades charcoal fragments, and in some cases risks loss of the entire sample (Knicker et al., 2007).

Pyrolysis is a third pretreatment option, which can be deployed after samples have undergone ABA or ABOx reactions. Pyrolysis removes hydrocarbon, polycyclic carbon, and other absorbed humic compounds by purging and then oxidizing released volatile compounds of the organic sample at 800 °C using Ar and O_2 gas, which converts organics into graphitic-like carbon black for AMS ^{14}C dating (Wang et al., 2010). The graphitic-like carbon black is the biomarker of carbon-carbon bonded aromatic molecules that are most resistant to weathering and biodegradation (Wang et al., 2003), and could be the ideal organic compound fraction for dating degraded charcoal fragments. However, pyrolysis requires large samples.

On arrival in the ISGS lab, Mochena Borago samples were dried and examined in preparation for pretreatment. At this stage, some samples appeared loose and crumbly while others retained some structural coherence. It was impossible to separate charcoal powders from the fine-grained sediments that accompanied them, either before or during pretreatment. Because samples were so small and fragmentary, there was not enough material to conduct high-dosed acid pretreatments such as ABOx. Therefore, the only suitable initial pretreatment was the standard acid-base-acid (ABA) method. By the end of ABA pretreatment, samples consisted of disseminated charcoal mixed with fine grained dark sediments, and had insufficient carbon for pyrolysis.

ISGS ABA pretreatment involves boiling for 1 h in 2 M HCl and rinsing to neutrality with DH_2O; soaking in cool 0.125 M NaOH for 1 h and rinsing to neutrality with DH_2O; soaking in 2 M HCl for 30 min and rinsing to pH 6 with DH_2O, and finally overnight drying in an 80 °C oven. ISGS ^{14}C-free wood background and wood working standard samplessamples, including including IAEA C5 (Two Creek forest wood), FIRI-D (Fifth International Radiocarbon Inter-comparison D wood), and ISGS Reiley AC (about 3 half-life wood) samples underwent the same pre-treatment (Wang et al., 2003).

ISGS charcoal samples, and wood background and working standards, are sealed with Cu granules in preheated quartz tubes for combustion (2 h at 800 °C). Then tubes are cooled from 800 °C to 600 °C for 6 h so Cu reduces the nitrogen oxides to nitrogen gas. Purified CO_2 is submitted to the University of California-Irvine's Keck Carbon Cycle AMS Laboratory for AMS ^{14}C analysis using the hydrogen-iron reduction method. All results undergo isotopic fractionation correction following Stuiver and Polach (1977), with AMS spectrometer measurement of δ^{13}C values on prepared graphite.

AMS results are examined to ensure that all ISGS working standards are within target values with 1–2 standard deviations. Background blanks are older than 53,300 ^{14}C bp with F^{14}C of 0.0013 (> 57,000 Cal BP; Hughen et al., 2006) against the internal background of the AMS facility. This suggests that charcoal samples with ^{14}C ages above 40 ka (e.g. 41,580 ^{14}C bp with F^{14}C of 0.0057 and 48,850 ^{14}C bp with F^{14}C of 0.0023) are true finite ages.

COL lab procedures are described in detail by Rethemeyer et al. (2013), and briefly reviewed here. Carbon extraction from charcoal proceeds via standard ABA extraction to remove inorganic carbon and humic substances (Rethemeyer et al., 2013 refer to this as 'acid–alkali–acid (AAA)' but it involves the same reagents used by ISGS above, albeit with different concentrations and reaction times). After acid extraction of the sample (1% HCl, ~10 h @ SRC), the residue is washed repeatedly with Milli-Q water (Millipore, USA). The alkali extraction (1% NaOH, 4 h, 60 °C) yields a non-soluble residue (humin) and an alkali-soluble fraction. From the latter, humic acids are precipitated via acidification (37% HCl to pH < 1); the precipitate is then rinsed with Milli-Q water to a pH of about 2. The humin fraction is washed repeatedly (Milli-Q water). Re-treatment (1% HCl ca. 10 h @ SRC) removes atmospheric CO_2 that might have been introduced during the alkali extraction, and is followed by a final rinse with Milli-Q water to pH > 4 (Rethemeyer et al., 2013).

Very small samples follow a modified carbon extraction procedure from that listed above, with reduced first acid extraction time – 1 h @ SRC – and no alkali extraction (Rethemeyer et al., 2013).

Sample combustion and graphitization uses advanced Automatic Graphitization Equipment linked to an Elementar VarioMicroCube elemental analyzer with a combustion tube (PbCrO4 and copper oxide) and a reduction tube (copper and silver wool). CO_2 from combustion enters a reactor of the AGE where the catalyst (H over Fe) converts it to graphite. Graphitized samples are stored in glass tubes filled with Ar to prevent contamination, and finally pressed into AMS target holders. To assure the quality of the sample handling and graphitization procedures, COL measures organic and bone standard materials selected from the Fifth Radiocarbon Intercomparison exercise (Rethemeyer et al., 2013).

3.3. Lab results and unmodeled calibration

Supplementary data Table A presents lab results in uncalibrated radiocarbon years, along with unmodeled individual calibrations via CalPal (the system we used in 2012) and IntCal (the system we use today). In this and all other tables and figures, dates are placed in their stratigraphic groups and then ordered according to the elevation of each sample.

4. Bayesian modeling methods and results

Applying Bayesian modeling to radiocarbon calibration has enhanced the precision of archaeological description and interpretation across the entire range of radiocarbon dating (Bayliss et al., 2015; Benazzi et al., 2011; Douka et al., 2014; Higham et al., 2006, 2011; Whittle et al., 2008). Since its initial use in archaeology (Buck et al., 1996), Bayesian modeling has steadily gained popularity as OxCal (Bronk Ramsey, 2001, 2009a) has become widely available and straightforward to operate.

The decisions an archaeologist makes while working with Bayesian models are far from simple, particularly when faced with complex stratigraphy or a significant proportion of "outlier" dates with various possible causes (Bayliss and Bronk Ramsey, 2004). Under such

circumstances, a thorough account of these decisions, and the logic underlying them, is essential (Bayliss, 2015).

We decided to use Bayesian models to calibrate the radiocarbon dates at Mochena Borago Rockshelter for two primary reasons. First, we hoped to identify potentially-outlying radiocarbon samples that may complicate the BXA's Pleistocene chronological sequence, to assist examinations of site formation and post-depositional processes. Second, we aimed to refine age estimates for the major lithostratigraphic units, to better assess how technological change at Mochena Borago fits into regional chronologies for MIS 3. To achieve these objectives, we first ran an initial model to help flag outlier dates, and then created a second, "cleaner" model that generated more precise estimates of the major chronostratigraphic units of the rockshelter. Codes for these models are presented in Supplementary data Table B (initial model) and Supplementary data Table C (clean model).

We used OxCal version 4.2 to construct and fit our Bayesian chronological model with IntCal13 as the calibration curve (Bronk Ramsey, 2009a; Reimer et al., 2013). We used default parameters for OxCal operation in most cases, and we built the model to include a 5% probability that any sample might be an outlier. All of the age ranges from our models are reported with 95.4% confidence intervals, including estimates for the beginning and ending of each major chronostratigraphic unit. Estimated means and standard deviations are also reported.

4.1. Principles of Bayesian modeling

Over the past five decades, scholars have continually refined the calibration of radiocarbon dates to compensate for fluctuations in atmospheric radiocarbon (Suess, 1967; Aitken, 1990; Weninger & Jöris, 2008; Reimer et al., 2013). However, calibrating dates individually – without a model that uses internal logic to impose constraints – can lead to needless imprecision due to statistical scatter (Bayliss, 2009: 130–132).

Bayesian modeling incorporates known stratigraphic relations between different radiocarbon samples into the calibration process, thereby improving precision (Buck et al., 1996: 215–218). By using stratigraphic evidence to model groups of radiocarbon dates into a relative chronology, the Bayesian approach can achieve narrower age ranges for individual dates within a sequence, and generate "simulated ages" for specific events during a site's formation, such as the beginning or end of a particular stratigraphic unit (Bayliss, 2009). It therefore provides the most benefit when applied to chronological sequences with direct stratigraphic links.

4.2. Application of Bayesian modeling to BXA Pleistocene deposits

Within the BXA, three contiguous 1 m² excavation squares (G10, G9, H9) contain six major Late Pleistocene lithostratigraphic units distinguished by obvious differences in the constituents and color of matrix and/or inclusions. Two of these are virtually sterile layers (YBT, YBS) that mark volcanic events. The other four major lithostratigraphic units (Lower T-Group, Upper T-Group, S-Group, and R-Group) have evidence for human occupation. These six major units, contiguous across excavation squares, are ideal "phases" that can be used to constrain a Bayesian model. (Minor stratigraphic subunits – which have more subtle distinctions, are non-contiguous, and therefore sometimes have ambiguous stratigraphic relations to each other – should not be used in this way.)

Bayesian modeling can establish concrete age estimates for each major lithostratigraphic group and volcanic event. This will clarify the late Pleistocene archaeology of Mochena Borago in several respects. First, it creates a secure chronological interval within which more localized site formation processes can be reconstructed (e.g. Meyer et al., n.d.). Second, it can establish precise ages for "benchmark" strata (such as YBT and YBS) that may be found in non-contiguous excavation units elsewhere in the rockshelter. Third, age ranges for major

lithostratigraphic units will aid in the dating of specific activities and behavioral changes at Mochena Borago, especially changes in stone tool technology.

Our application of Bayesian modeling to Mochena Borago began by using the contiguous strata documented within the BXA to constrain models for ages. In our model, each major lithostratigraphic unit (e.g., Upper T-Group) was a discrete phase, and consecutive stratigraphic units were consecutive phases (Lower T-Group deposition must precede Upper T-Group deposition).

Before attempting to run the model, we were forced to exclude two dates (Table 2, third-last column). Samples SWAP12-02 and SWAP12-05 both yielded ^{14}C ages >49 ka. Because the samples had sufficient carbon mass after burning, the infinity dates most likely reflect the fact that the samples are older than the limits of radiocarbon dating. Such dates cannot be calibrated and therefore cannot be accommodated in a Bayesian model for radiocarbon.

4.3. Detecting outliers, and modeling their probabilities

Bronk Ramsey (2009b) defines four different types of problems affecting radiocarbon dates: S, R, D, and T. Type S errors result from incorrect measurement of the ^{14}C sample; reported lab errors, which typically follow a normal distribution around a central age estimate, might not accurately reflect the possible variance in true age. Type R errors result from reservoir effects such as marine offsets, carbon recycling in lacustrine organisms, or ingestion of dead carbon for ostrich eggshell formation; these yield dates that are older than expected for the context. Type D errors occur across a group of samples, when multiple individual dates derived from similar or related sources are collectively subject to errors of Type S or Type R. Type T anomalies are not errors but outliers, which reflect a mismatch between the event being dated and the sample being measured. These can occur in two ways: the material being dated may belong to the context but ultimately derive from an earlier time (old wood), or postdepositional processes may introduce material from later or earlier events into the context under examination (taphonomic).

Outliers – dates that deviate substantially from stratigraphically-based expectations – become apparent at two different stages in Bayesian analysis. Some outliers manifest themselves by "crashing" the model: their calibrated age ranges are so extremely incompatible with the stratigraphic phases the researcher built into the model that OxCal simply refuses to complete it. The researcher then must either reconsider stratigraphic relations or, if those are solid, exclude the incompatible dates and re-attempt the model. Other outliers may be less extreme: dates may be compatible enough with the model to allow it to run to completion. However, the model output statistics will show serious discrepancies between the dates' calibrated ages and those that the model predicted. Any decision to exclude a date must consider the outlier's possible causes.

Initial attempts to run the model failed due to extreme outliers in T-Group: Samples SWAP14-01, SWAP14-02, SWAP14-03, and SWAP14-09 all yielded dates that are much younger than those from overlying strata. Because these anomalous dates are all isolated within two closely related minor stratigraphic units (AED and AEC) in the northwest quadrant of excavation unit H9, we believe they are a Type T outlier caused by a postdepositional taphonomic event. We were forced to exclude all these samples in order for the initial model to run successfully (Table 2, second to last column).

4.4. Initial Bayesian modeling of phases in the Block Excavation Area (BXA)

Our initial run of OxCal 4.2 proposed six successive phases representing the six major Pleistocene lithostratigraphic groups in the BXA: Lower T-Group, Upper T-Group, YBT, S-Group, YBS, and R-Group. It included all dates that were <49 kbp and allowed the OxCal run to complete (Table 2, second-last column). The model assumed that a

Table 2

Radiocarbon age determinations from Illinois Geological Survey (ISGS) and University of Cologne (COL). On the right side of the table, columns denote inclusion in various stages of modeling attempts: <49 ka (third-last column), allowing the initial model to succeed (second-last column), and meeting the convergence (C) and probability (P) criteria for inclusion in the final model (last column).

Sample #	Bag #	Lab #	Excavation unit	Level	Major strat group	Minor strat subunit	Elev (m)	^{14}C bp	d^{13}C	<49 k?	Initial model	Clean model
SWAP08-11	3424	ISGS-A1227	G9	4	Upper R	RCA	2213.798	37,200 ± 560	−21.1	Yes	Yes	Yes
SWAP08-07	2141	ISGS-A1063	H9	15	Upper R	RCA	2213.756	36,120 ± 590	−24.8	Yes	Yes	Yes
SWAP08-08	2237	ISGS-A1064	H9	15	Upper R	RCA	2213.743	33,370 ± 420	−22.2	Yes	Yes	Yes
SWAP07-03	2200	ISGS-A1024	H9	15	Upper R	RCA	2213.740	35,010 ± 270	−23.7	Yes	Yes	Yes
SWAP08-10	3834	ISGS-A1226	G9	5	Upper R	RCA	2213.709	34,360 ± 400	−23.6	Yes	Yes	Yes
SWAP08-12	2804	ISGS-A1228	H9	18	Upper R	RCA	2213.657	36,900 ± 540	−25.5	Yes	Yes	Yes
SWAP07-05	2596	ISGS-A1015	H9	18	Upper R	RCA	2213.630	37,930 ± 370	−23.3	Yes	Yes	Yes
SWAP10-01	11105	COL2367.1.1	G9	11	Lower R	RGCM	2213.663	36,108 ± 220	−27.2	Yes	Yes	Yes
SWAP14-11	11830	COL2368.1.1	G9	12	Lower R	RGCB	2213.647	37,861 ± 247	−26.8	Yes	Yes	Yes
SWAP08-05	3346	ISGS-A1062	H9	19	Lower R	RGCA	2213.624	40,500 ± 1000	−25.2	Yes	Yes	
SWAP07-06	3334	ISGS-A1013	H9	19	Lower R	RGCA	2213.621	41,580 ± 590	−22.9	Yes	Yes	
SWAP08-09	2248	ISGS-A1225	G10		YBS	YBS	2213.527	38,750 ± 680	−25.1	Yes	Yes	Yes
SWAP14-13	14808	COL2370.1.1	G9	15	YBS	YBS	2213.518	39,914 ± 276	−23.8	Yes	Yes	Yes
SWAP14-12	14835	COL2369.1.1	G9	15	YBS	YBS	2213.516	37,847 ± 246	−27.6	Yes	Yes	
SWAP07-07	4039	ISGS-A1014	H9	26	S-group	VDBS	2213.375	39,200 ± 440	−28.9	Yes	Yes	
SWAP08-04	4002	ISGS-A1057	H9	26	S-group	VDBS	2213.365	44,000 ± 1600	−23.9	Yes	Yes	Yes
SWAP12-02	33228-A	COL1833.1.1	G9 NE	52	S-group	ABA	2213.148	>49,000	−28.5			
SWAP12-01	33228-B	ISGS-A2261	G9 NE	52	S-group	ABA	2213.148	45,470 ± 2180	*	Yes	Yes	Yes
SWAP08-03	2037	ISGS-A1060	G10	17	YBT	YBT main	2213.185	36,960 ± 650	*	Yes	Yes	
SWAP07-09	2105	ISGS-A1019	G10	17	YBT	YBT main	2213.116	41,830 ± 600	−26.8	Yes	Yes	Yes
SWAP14-04	17058	COL2333.1.1	H9 NE	50	YBT	YBT-SCS	2213.028	42,347 ± 337	−24.7	Yes	Yes	Yes
SWAP14-05	17082	COL2334.1.1	H9 NE	53	YBT	YBT-SCS	2212.992	42,842 ± 362	−21.8	Yes	Yes	Yes
SWAP08-02	2109	ISGS-A1059	G10	18	Transition	YBT/DCC	2213.008	47,700 ± 2500	−23.3	Yes	Yes	Yes
SWAP07-11	2117	ISGS-A1017	G10	19	Upper T	DCC	2212.975	42,400 ± 650	−23.7	Yes	Yes	Yes
SWAP12-04	33380-A	COL1834.1.1	G9 NE	66	Upper T	ADD	2212.913	43,284 ± 1058	−25.9	Yes	Yes	Yes
SWAP12-03	33380-B	ISGS-A2262	G9 NE	66	Upper T	ADD	2212.913	40,210 ± 980	*	Yes	Yes	Yes
SWAP12-05	33404	COL1835.1.1	G9 NE	68	Upper T	ADD	2212.880	>49,000	−25.6			
SWAP07-12	3112	ISGS-A1018	G10	23	Upper T	DCC	2212.840	39,920 ± 480	−22.2	Yes	Yes	
SWAP14-08	30456-B	COL2337.1.1	G9SE	67	Upper T	ACY	2212.812	45,341 ± 425	−23.4	Yes	Yes	Yes
SWAP14-07	33458	COL2336.1.1	G9 NE	70	Upper T	ADD	2212.812	45,182 ± 427	−22.6	Yes	Yes	Yes
SWAP14-01	29996	ISGS-A3129	H9 NW	104	Upper T	AEC	2212.767	24,270 ± 150	−20.7	Yes		
SWAP08-01	3135	ISGS-A1058	G10	24	Upper T	DCC	2212.743	26,400 ± 180	−24.3	Yes	Yes	
SWAP07-13	3123	ISGS-A1025	G10	25	Lower T	CTT	2212.780	48,850 ± 1420	−24.2	Yes	Yes	Yes
SWAP14-09	36618	COL2720.2.1	H9	108	Lower T	AED	2212.718	33,891 ± 295	−23.1	Yes		
SWAP14-03	36654	ISGS-A3113	H9 NW	109	Lower T	AED	2212.679	25,720 ± 140	−21.4	Yes		
SWAP14-06	33706	COL2335.1.1	G9 NE	75	Lower T	ADM	2212.664	48,102 ± 536	−16.5	Yes	Yes	Yes
SWAP14-02	37317	ISGS-A3131	H9SW	110	Lower T	AED	2212.639	35,720 ± 470	−23.1	Yes		

* denotes samples with an insufficient amount of carbon for δ^{13}C analysis.

clear boundary existed between each phase, and generated a series of probable age ranges for the start and end of each phase (95.4% probability). Outputs for the initial model run appear as Fig. 4 (probability curves) and Supplementary data Table D (data).

We then examined the model outputs for dates that might be classified as "outliers" based on various diagnostic criteria from OxCal: Agreement index (A), Convergence of the Markov-Chain Monte Carlo algorithm (C), and Probability of not being an outlier (P) (Bronk Ramsey, 2009b). Several dates looked dubious because of a low Agreement Index value (A < 60). Of these, however, only a few failed the MCMC convergence test (C < 95%). We decided to exclude all of the MCMC failures. We then examined the spread of posterior probabilities of not being an outlier (P), and decided to exclude any date with P < 50. This excluded four additional dates beyond those already excluded for poor convergence. All other dates were included in the final, "clean" model (Table 2, final column). Details on the identification of each outlier are presented below; see also Fig. 4 and Supplementary data Table D.

Lower T-Group dating samples included in the initial model were SWAP14-06 (P = 98.0) and SWAP07-13 (P = 96.8). Both could be included in the final model.

Upper T-Group samples included in the initial model were SWAP08-01 (P < 0.1), SWAP14-07 (P = 88.5), SWAP14-08 (P = 85.5), SWAP07-12 (P < 0.1), SWAP12-04 (P = 97.4), SWAP12-03 (P = 61.2), and SWAP07-11 (P = 88.1). Samples 12-03 and 12-04 were modeled together as a single date because both should have the same calendar age as they were split from a single specimen and processed at separate

labs. The initial model run revealed two outliers. SWAP 08-01 (A = 5.5, C = 96.9, P < 0.1) is more than 10,000 years later than other Upper T dating samples; coming from the easternmost portion of square G10, we must consider that the taphonomic processes affecting substrata AEC and AED also may have operated here. SWAP 07-12 (A = 5.3, C = 96, P < 0.1) is another likely Type T outlier, with an unmodeled age range several thousand years later than other dates in this lithostratigraphic group.

YBT yielded five radiocarbon samples, all of which were included in the initial model: SWAP08-02 (P = 77.8), SWAP14-05 (P = 98.5), SWAP14-04 (P = 98.6), SWAP07-09 (P = 97.5), and SWAP08-03 (P < 0.1). The model run revealed one Type T outlier: SWAP08-03 (A = 5.5, C = 98.8, P < 0.1) from near the top of YBT, has a date that is younger than expected.

S-Group had three samples that could be included in the model, which yielded highly variable calibrated age ranges. SWAP07-07 (A = 14, C = 97.9, P = 40.1) is much younger than the model predicts from other samples in its depositional groups, and thus may represent an intrusion. The remaining two samples – SWAP12-01 (P = 78.6) and SWAP08-04 (P = 87.7) – have age ranges older than expected, but P indices high enough to be retained for the final model. The marked variation in S-Group dates is not surprising given fluvial activities documented during excavation. Phase modeling for S-Group is heavily constrained by neighboring strata (YBT below, and YBS above) each of which has an internally consistent set of dates.

YBS deposits yielded three samples that could all be included in the initial model: SWAP14-12 (P = 41.4), SWAP14-13 (P = 91.4), and

Fig. 4. Plotted probability curves (95.4%) for the initial model run with 31 dates included. Pale grey curves show unmodeled probability curves for calibrations; dark grey curves show modeled probability curves for calibrations. Outliers are marked with an X on the right side.

SWAP08-09 ($P = 97.6$). SWAP14-12 ($A = 26.7$, $C = 90$, $P = 41.4$) is a Type T outlier (too young, likely intrusive material).

R-Group deposits furnished eleven dates that were all included in the initial model: SWAP07-06 ($P = 0.8$), SWAP08-05 ($P = 37.9$), SWAP14-11 ($P = 96.6$), SWAP10-01 ($P = 96.8$), SWAP07-05 ($P = 96.6$), SWAP08-12 ($P = 97.3$), SWAP08-10 ($P = 91.8$), SWAP07-3 ($P = 94.4$), SWAP08-08 ($P = 62.4$), SWAP08-07 ($P = 97.1$), SWAP08-11 ($P = 97.3$). The initial model identified two outliers that yielded unexpectedly old age ranges: SWAP 08-05 ($A = 14.7$, $C = 91.4$, $P = 37.9$) and SWAP 07-06 ($A = 5.4$, $C = 91.6$, $P = 0.8$). They are from the same excavation unit and level.

Although it is unusual for post-depositional processes to introduce *older* materials, we are considering at least four possible causes for Type T outliers in cases where the charcoal ^{14}C ages may be older than the strata they were recovered from:

1. In the eastern area of the rockshelter, excavation units N42E35 and N42E36 have exposed strata ^{14}C dated on charcoal to >49 ka that are higher in elevation than BXA's T, YBT and S-Group deposits. Therefore, material from eastern deposits, including charcoal, could have been dislodged and displaced into the BXA through colluvial, fluvial, or erosional processes, and/or bioturbation or anthropogenic activities.
2. P. Goldberg (pers. comm.) and Meyer et al. (n.d.) allude to several likely episodes of water saturation within the BXA sequence (e.g., ponding and slow-moving streams) that may have caused the loosening or erosion of sediments. In such circumstances, lower and older strata may have released charcoal into the water, and charcoal may have floated to the surface and redeposited at the contact between the water surface and younger deposits.
3. Within the BXA, vertical transport of charcoal could have occurred through bioturbation, including burrowing by insects, terrestrial crabs (observed live during excavations) and rodents and other small mammals.
4. Similarly, humans could have disrupted depositional sequences by creating hearths or digging artificial pits, thereby moving long-buried material onto a younger occupational surface.

4.5. Final Bayesian modeling of phases for BXA sequence, with outliers removed

Having identified major outliers and evaluated their possible causes, we follow Bronk Ramsey's (2009b) suggestion to run a "clean" version of the Bayesian model using dates that both satisfy recommended convergence values and also have >50% probability of having ages that reflect the age of their major stratigraphic group (Table 2, final column). Outputs for the final model appear in Fig. 5 (probability curves for modeled dates and phases) and Table 3 (supporting data, including mean and standard deviation estimates for each date). Final age ranges (95.4% probability) for the start and end dates of each major stratigraphic group are summarized and compared to earlier weighted mean calculations in Table 4.

5. Discussion

Initial publication of the BXA Late Pleistocene sequence was based upon five seasons of excavation, 22 radiocarbon dates, and the use of weighted means to express likely age ranges for major lithostratigraphic units (Brandt et al., 2012; Fisher, 2010). Since then, four more field seasons, 15 new dates, and additional analytical methods have considerably expanded our knowledge base. In the following sections we provide an overview for each major stratigraphic group of the ways in which Bayesian modeling has permitted us to: 1) revise previous age ranges; 2) identify and consider potential causes of outlier dates; and 3) reconsider old and develop new ideas concerning changes in lithic technology and other aspects of behavior.
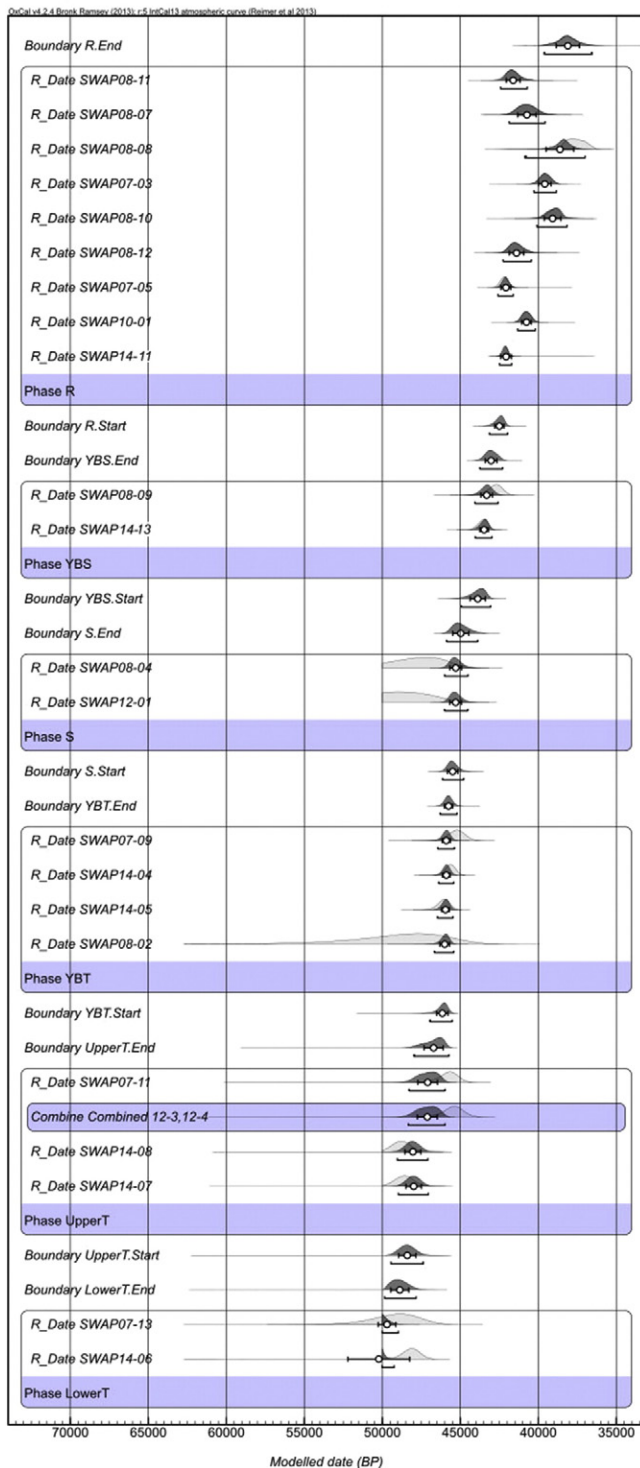
Fig. 5. Plotted probability curves (95.4%) for the clean model run (outliers excluded).

5.1. Revised age range

Comparisons between weighted means and Bayesian age models are complicated by the fact that an "age range" derived from a weighted mean calculation represents a normal, unimodal distribution around a central point of maximum probability, whereas a phase's age range derived from Bayesian modeling incorporates two probability curves – one for the start of the phase, and one for its end – which are not necessarily normal. Therefore, for discussion purposes we have converted our

previously published weighted mean ranges with 1-sigma errors (Brandt et al., 2012) into age ranges reflecting 2-sigma confidence intervals to allow for easier comparison. With the exception of the 2012 weighted mean calculations based on CalPal calibrations, all ^{14}C dates mentioned in the following sections are calibrated using IntCal 13 unless otherwise noted.

5.2. Outliers

Bayesian modeling provides a statistical rather than "cherry picked" reason for rejecting certain dates, and can serve as a starting point for discussions about why particular samples yield dates that deviate from expected values. Single to multiple processes merit consideration as potential causal mechanisms: 1) bioturbation (e.g., via root growth or animal burrowing); 2) mechanical displacement (e.g., fluvial or colluvial action); 3) chemical processes (e.g., leaching of original carbon or contamination with carbon from a different source); 4) geoturbation (e.g., eroded or reworked sediments); and 5) human activities (e.g., pits or substructures) (Meyer et al., n.d.; Taylor and Bar-Yosef, 2014). Detailed hypotheses and explanations for outlier causes are beyond the scope of this article, but below we offer initial suggestions designed to galvanize future research.

5.3. Lithic technological change

Brandt et al. (2012) observed that some lithic patterns underwent incremental change (e.g., small changes in raw material preferences, slight deviations in the dominance of Tabular SDM core reduction strategies), while others remained at stasis for ~20,000 years (e.g., retention of Levallois core reduction at low frequencies). Therefore, revising BXA's chronology cannot fundamentally reshape our current ideas about temporal changes in lithic technology. Instead the new chronology gently stretches the temporal frame, suggesting that continuities and changes in lithic technology spanned a longer period than previously thought. Because the modeled age ranges reveal the true degree of uncertainty about "start" and "end" dates for major phases, they may inject a much-needed note of caution into efforts to pinpoint dates for specific innovations, or correlate particular behavioral changes with external shifts in environment. Nevertheless, a few significant technological developments require updating in light of revised age ranges and continued lithic analyses of BXA assemblages since 2012.

5.4. Lower T-Group: >50 ka to 49.9–47.8 ka

5.4.1. Revised age range

The single date available in 2012, calibrated by CalPal to 2-sigmas, indicated a range of 58.4–48.0 ka for Lower T-Group. Unfortunately research since then has not led to any greater precision in defining the beginning of T-Group deposition, as 20–30 cm of sediments at the base of Lower T-Group still remain undated due to the absence of charcoal. We can only conclude that Lower T-Group deposits began to accumulate both through natural and human-derived events sometime before 50 ka. Our Bayesian model (now based on two dates) suggests that Lower T-Group deposition ended between 49.9 and 47.8 ka, which is reasonably concordant with weighted mean calculations.

5.4.2. Outliers

Three ^{14}C dates of ~31 ka, ~39 ka and ~41 ka from sub-stratum AED in Unit H9 indicate that a postdepositional event – possibly bioturbation – brought small pieces of charcoal and perhaps other material down into certain strata within Lower T-Group. Although lithics from the sub-stratum encompassing the intrusive charcoal (AED) are fresh and show no signs of abrasion, planned lithic studies will isolate these from the other Lower T-Group assemblages for comparative purposes.

Table 3

Output data file for the final run of the "clean" model (with the outliers excluded).

Name	Unmodeled (BP)					Modeled (BP)					Diagnostic criteria		
	From	To	%	mu	Sigma	From	To	%	mu	Sigma	A	C	P
Boundary R.End						39,623	36,557	95.4	38,109	744		94.2	
Span R						2426	4983	95.4	3751	622		99	
R_Date SWAP08-11	42,544	40,729	95.4	41,668	445	42,415	40,710	95.4	41,615	441	104.6	99.4	96.1
R_Date SWAP08-07	41,860	39,579	95.4	40,731	582	41,870	39,566	95.4	40,732	589	101.2	99.3	95.9
R_Date SWAP08-08	38,637	36,475	95.4	37,609	583	40,864	37,002	95.4	38,615	887	64.6	98.5	84.1
R_Date SWAP07-03	40,206	38,870	95.4	39,547	341	40,281	38,845	95.4	39,585	402	100.3	99.4	95.3
R_Date SWAP08-10	39,907	38,035	95.4	38,927	458	40,088	38,163	95.4	39,087	528	98.2	99.4	94.6
R_Date SWAP08-12	42,299	40,444	95.4	41,422	463	42,256	40,450	95.4	41,400	466	102.5	99.5	96.1
R_Date SWAP07-05	42,718	41,684	95.4	42,199	257	42,583	41,610	95.4	42,079	313	103.4	99.5	95.6
R_Date SWAP10-01	41,301	40,216	95.4	40,761	279	41,325	40,194	95.4	40,761	304	100.9	99.5	96
R_Date SWAP14-11	42,530	41,775	95.4	42,151	188	42,486	41,710	95.4	42,069	340	102.1	99.6	95.4
Phase R													
Boundary R.Start						43,134	41,972	95.4	42,498	296		99.9	
Boundary YBS.End						43,746	42,291	95.4	43,028	372		99.7	
Span YBS						0	871	95.4	274	276		99.9	
R_Date SWAP08-09	43,970	41,851	95.4	42,820	524	44,061	42,581	95.4	43,312	369	73.6	99.8	95.8
R_Date SWAP14-13	44,168	43,021	95.4	43,566	293	44,038	42,977	95.4	43,477	269	105	99.9	96.5
Phase YBS													
Boundary YBS.Start						44,935	43,061	95.4	43,884	486		99.6	
Boundary S.End						45,879	43,885	95.4	44,973	510		99.3	
Span S						0	578	95.4	155	191		100	
R_Date SWAP08-04	…	45,289	95.4	47,460	1316	46,003	44,512	95.4	45,293	375	47	99.9	94.4
R_Date SWAP12-01	…	45,803	95.4	48,048	1244	46,010	44,522	95.4	45,299	375	18.2	99.8	92
Phase S													
Boundary S.Start						46,136	44,790	95.4	45,493	336		99.8	
Boundary YBT.End						46,293	45,210	95.4	45,754	267		99.7	
Span YBT						0	810	95.4	244	270		99.9	
R_Date SWAP07-09	46,382	44,196	95.4	45,261	544	46,441	45,379	95.4	45,902	263	65.2	99.9	95.7
R_Date SWAP14-04	46,305	44,995	95.4	45,642	327	46,387	45,422	95.4	45,899	241	92.7	99.9	96.4
R_Date SWAP14-05	46,859	45,344	95.4	46,075	380	46,463	45,472	95.4	45,953	248	118.7	99.9	96.9
R_Date SWAP08-02	56,957	43,513	95.4	49,320	3455	46,658	45,422	95.4	46,001	311	106.3	99.9	89.3
Phase YBT													
Boundary YBT.Start						46,939	45,523	95.4	46,155	360		99.5	
Boundary Upper T.End						47,965	45,735	95.4	46,714	610		99.5	
Span Upper T						0	2504	95.4	1268	750		99.5	
R_Date SWAP07-11	47,117	44,585	95.4	45,792	632	48,287	45,983	95.4	47,094	631	30.9	99.5	90.4
R_Date SWAP12-03	45,726	42,489	95.4	44,034	848	48,332	45,986	95.4	47,117	637	3.1	99.5	78.8
R_Date SWAP12-04	49,215	44,881	95.4	46,860	1104	48,332	45,986	95.4	47,117	637	113.8	99.5	96.1
Combined 12-3,12-4	46,942	44,187	95.4	45,496	682	48,332	45,986	95.4	47,117	637		99.5	
R_Date SWAP14-08	49,882	47,740	95.4	48,777	551	49,035	47,083	95.4	48,041	509	67.3	99.6	93
R_Date SWAP14-07	49,751	47,497	95.4	48,605	570	48,968	47,055	95.4	47,991	495	80.8	99.6	94.2
Phase Upper T													
Boundary Upper T.Start						49,445	47,375	95.4	48,401	550		99.5	
Boundary Lower T.End						49,853	47,836	95.4	48,880	578		99.1	
R_Date SWAP07-13	52,505	46,348	95.4	49,270	1568	50,005	48,973	95.4	49,701	561	123	97.4	95.6
R_Date SWAP14-06	49,256	47,093	95.4	48,156	543	50,017	49,245	95.4	50,226	1981	2.3	96.6	92.7
Phase Lower T													
Sequence BXA													
U(0,4)	3.99E−17	4	95.4	2	1.1431	5.38E−17	3.94	95.5	2.33465	1.1455	100	82.2	
T(5)	−2.65	2.65	95.4	−2.27E-08	1.2908				0.32978	1.842		98.3	
Outlier model general						−3467	4628	95.4	544	2136		99.5	

5.4.3. Lithic technological change

The lithics from Lower T-Group, and for that matter all the stratigraphic groups at Mochena Borago, share a distinctive combination of core reduction strategies, tool types and other artifacts, that do not match any other known site in the Horn of Africa. Nor is this combination easy to place within traditional culture-historic stages such as the MSA or LSA (Brandt et al., 2012). For example, despite the presence of Nubian cores and points in the T-Group and overlying deposits, it is unlikely that Mochena Borago's lithic tradition derives from the Nubian Complex. The origin of Mochena Borago's distinct lithic tradition remains unknown until further excavations at Mochena Borago or other sites in the region can provide sequences chronometrically dated to earlier than 50 ka.

Recent analyses of previously unstudied Lower T-Group assemblages have documented backed pieces for the first time (R. Vogelsang pers. obs.). Ranging from >50 to 48 ka in age based on the Bayesian model, these backed pieces, albeit few in number, represent the oldest securely dated evidence for purposeful blunting of flake and blade edges in the Horn. Whether backed pieces served as arrow armatures is a subject of great debate. The recent discovery of plant and animal residues as well as traces of use wear on >200 artifacts from Lower and Upper T-Groups, including backed pieces, promises to shed new light on the functions of stone tools >50–40 ka (C. Lentfer and V. Rots pers. comm.).

5.5. Upper T-Group: 49.4–47.4 ka to 48.0–45.7 ka

5.5.1. Revised age range

Weighted mean calculations from the three dates available in 2012 yielded a 2-sigma range of 47.1–43.2 ka for Upper T-Group. Bayesian modeling suggests a start date sometime between 49.4 and 47.4 ka, 2000 years earlier than previously thought. End dates for Upper T-

Table 4
Comparison of age ranges for major stratigraphic groups in the BXA. Rows with grey fill represent hiati in rockshelter use during major volcanic events. Weighted means (after Brandt et al., 2012) are presented on the left-hand three columns. Start and end dates for major stratigraphic groups based on the "clean" Bayesian model (outliers excluded) appear on the right side of the table. All dates are Cal BP.

14C dates available in 2012 (#)	Weighted mean (1σ)	Weighted mean age range: (2σ) Start	End	Strati–graphic Group	14C dates now available (#): In clean model Total	model	Bayesian model BP age range for **start** of phase (2σ)	Bayesian model BP age range for **end** of phase (2σ)
11	41,159 ± 783	42,700	39,600	**R–Group**	11	9	43,134–41,972	39,623–36,557
1	43,121 ± 692	44,500	41,800	**YBS**	3	2	44,935–43,061	43,746–42,291
3	43,480 ± 443	44,300	42,600	**S–Group**	4	2	46,136–44,790	45,879–43,885
3	43,403 ± 1213	45,800	41,000	**YBT**	5	4	46,939–45,523	46,293–45,210
3	45,164 ± 982	47,100	43,200	**Upper T**	9	5	49,445–47,375	47,965–45,735
1	53,224 ± 2662	58,400	48,000	**Lower T**	5	2	*No model age*	49,853–47,836

Group, modeled as 48.0–45.7 ka, are at least 2500 years earlier than the youngest age anticipated by weighted means.

5.5.2. Outliers

Two dates of ~30.5 ka and ~28 ka (unmodeled IntCal calibration; see Supplementary Data Table A) are significantly younger than expected, and were rejected by the Bayesian model. These were probably intrusive due to one or more of the aforementioned potential causes. The single date of >49 ka within Upper T-Group is too old to be incorporated into the Bayesian model, and also constitutes an outlier. Section 4.4 discusses potential causes for unexpectedly old dates.

5.5.3. Lithic technological change

Lithics from Upper T-Group show many of the same characteristics as those in Lower T-Group. Unifacial and bifacial points made mostly on elongated flakes from Tabular SDM cores still form the highest percentage of shaped tools, but backed pieces now represent the second highest percentage at the expense of points. Although sample sizes are small, it is tempting to view these shifts in frequency as reflecting changing perspectives on the importance of points vs. backed tools as composite tool armatures.

5.6. YBT tephra: 46.9–45.5 ka to 46.4 ka–45.4 ka

5.6.1. Revised age range

In 2012, weighted mean calculations from three dates suggested that deposition of this tephra occurred sometime between 45.8–41.0 ka. Bayesian modeling suggests a start date sometime between 46.9 and 45.5 ka, and an end date sometime between 46.3 and 45.2 ka. Because tephra deposition was probably a very brief event (i.e. start and end dates for this tephra should be <100 years apart) we can narrow the range further: YBT deposition probably started after 46.4 ka, and ended by 45.4 ka.

5.6.2. Outliers

Dates are mostly consistent through YBT, as one might expect in a tephra. However its upper reaches have one outlier (~42.5–40 ka, unmodeled IntCal calibration) that suggests contamination from later fluvial processes. This has little impact on artifact analysis, because YBT is for all practical purposes archaeologically sterile.

5.7. S-Group: 46.1–45.4 ka to 45.8–43.9 ka

5.7.1. Revised age range

Weighted mean calculations from three dates in 2012 had given a 2-sigma range of 44.3–42.6 ka for S-Group. Bayesian modeling suggests a start date sometime between 46.1 and 44.8 ka, again allowing for a substantially earlier onset. The brief nature of YBT deposition might argue for an even narrower and earlier S-Group start range (i.e. 46.1–45.4 ka); however this would assume that S-Group reoccupation followed immediately on the heels of the YBT eruption, which is unlikely given the major unconformity on the YBT/S-Group interface. End dates for S-Group, modeled as 45.8–43.9 ka, are at least 1200 years earlier than the youngest age anticipated by weighted means.

5.7.2. Outliers

Since the charcoal dating to 43.8–42.3 ka (unmodeled IntCal calibration) was eliminated from the model, this sample should be considered intrusive. Whether it originated from overlying YBS, or less likely R-Group deposits, or was brought in via the paleofluvial channel, remains uncertain. The charcoal dating to >49 ka represents the uppermost sample beyond calibration, and within the context of S-Group must be seen as an outlier.

5.7.3. Lithic technological change

S-Group lithics reveal a number of important differences with the earlier T-Group assemblages. Whereas T-Group lithics are virtually all fresh, S-Group deposits witness a significant increase in the number and percentage of lithics with varying degrees of abrasion and rolling indicative of geoturbation. Nevertheless, >80% are fresh and nearly 100% are obsidian – another change from the T-Group where assemblages always maintain a very low but consistent percentage of non-volcanic or silicious artifacts. The significant increase in the frequency of bipolar cores in the S-Group is one of the more notable changes in the BXA archaeological sequence. Why this technology is more prevalent in S-Group assemblages is not yet understood, particularly when knappers presumably had access to excellent, plentiful obsidian from Baantu and perhaps other sources. Research into African bipolar reduction strategies has recently experienced a surge in interest (e.g. Hiscock, 2015), and plans are afoot to develop more detailed studies of Mochena Borago samples in future seasons.

5.8. YBS mudflow: 44.9–43.1 ka to 43.7–42.3 ka

5.8.1. Revised age range

The single date available for YBS in 2012, calibrated by CalPal, had suggested that deposition of this pyroclastic mudflow occurred sometime between 44.5–41.8 ka. Bayesian modeling suggests a start date sometime between 44.9 and 43.1 ka, and an end date sometime between 43.7 and 42.3 ka. Like YBT, the YBS mudflow probably spanned a period of <100 years, so its deposition should not have started before 43.8 ka, and should not have ended after 43.0 ka.

5.8.2. Outliers

During the YBS mudflow, fluvial processes brought natural material into the rockshelter. There was thus potential for pre-existing archaeological material to have been picked up by the mudflow and integrated into YBS, but this did not happen: YBS contains only a few lithics, and the sole statistical outlier among its dating samples is only slightly too young. Its age range (42.5–41.8 ka via unmodeled IntCal calibration) still overlaps with the YBS's overall modeled age range.

5.9. R-Group: 43.1–42.0 ka to 39.6–36.6 ka

5.9.1. Revised age range

In 2012, weighted mean calculations from eleven dates suggested a 2-sigma range of 42.7–39.6 ka for R-Group. Bayesian modeling produces a start date sometime between 43.1 and 42.0 ka, roughly in line with the weighted mean. End dates, modeled as 39.6–36.6 ka, allow R-Group deposition to continue 3000 years later than anticipated by weighted means.

5.9.2. Outliers

R-Group deposits contain a puzzling pair of outliers that are older than the model suggests (46.1–44.0 ka and 46.0–42.6 ka, unmodeled IntCal calibrations). There is no evidence for bioturbation that would have transported materials up from deeper layers within the BXA. However, recent excavations in eastern parts of the shelter have revealed earlier deposits at higher elevations, from which charcoal could have moved laterally and down into the BXA during wet or erosional episodes. Future work in eastern Mochena Borago will clarify its chronology and examine the possibility of such transport.

5.9.3. Lithic technological change

R-Group lithics are reported here for the first time as they were not discussed in Brandt et al., 2012. One of the biggest and most puzzling aspects of its assemblages is the very high percentage of lithics that show some degree of abrasion or rolling – >65%! But the R-Group's matrix reveals little if any evidence for high-velocity fluvial action – the usual cause of artifact erosion. How, then, could only a third of the lithics be fresh? Or, conversely, why aren't all of the lithics abraded or rolled? Recent studies of the R-Group (and S-Group) assemblages have begun to address this question by giving special emphasis to analytically differentiating fresh vs. abraded artifacts (Bermensolo, 2013; Parow-Souchon et al., n.d.). Future research will use 3-D plot data to look for spatial and temporal patterns of fresh vs. damaged artifacts in a GIS framework.

Bayesian modeling has unexpected implications for the damaged condition of many R-Group lithics, when considered alongside the major unconformity and temporal hiatus of >26,000 years separating the youngest R-Group sediments from the early Holocene BWT tephra. Mochena Borago finds a parallel at Goda Buticha Cave, the only other Ethiopian site with stratified, chronometrically dated archaeological deposits spanning the last half of the Late Pleistocene. Goda Buticha's 48,000 year sequence is also disrupted by a major depositional and occupational gap from ~35 ka to ~8 ka (Pleurdeau et al., 2014). Weighted means (Brandt et al., 2012) had placed the latest levels of R-Group at ~40 ka, 5000 years earlier than the beginning of Goda Buticha's hiatus. Our new modeled age ranges reposition Mochena Borago's hiatus

from ~36 ka to ~8 ka, now making it contemporary with Goda Buticha's hiatus. Although so far only two sites demonstrate this Late Pleistocene depositional gap, we propose the working hypothesis that it corresponds to a sudden, major regional climatic event, in which arid and cold conditions triggered human demographic shifts and abandonment of some sites prior to the onset of the MIS 2 and the LGM.

5.10. A collective consideration of outliers

Of the thirty-seven dates obtained thus far for BXA Late Pleistocene deposits, twenty-four are consistent with the framework of the model and the overall stratigraphic sequence. Thirteen dates appear to be outliers, and it may be useful to discuss the extent to which these can be grouped into discrete events, episodes, or processes. Some of these may relate to observed formation processes, but others may relate to undetectable taphonomic events or even reflect sample contamination that could not be cleared via the gentle ABA preparation necessitated by small sample size. Reviewing possible explanations for particular sets of outliers, we can dismiss some and retain others for further investigation.

Lower and Upper T-Group deposits yielded five outliers (SWAP14-02, SWAP14-03, SWAP14-09, SWAP18-01, and SWAP14-01) and possibly a sixth (SWAP07-12) (Table 2). These five dates are much younger than their neighbors – a difference greater than 10,000 years! One possible explanation is sample contamination, but even if samples had been of sufficient size to use a more aggressive pretreatment regimen (e.g., ABOx) it is not clear whether this degree of discrepancy could be remedied – and even if it could, one would also have to explain why such contamination affected this group of samples so selectively. Because the five samples are from two adjacent minor strata that are spatially circumscribed, it is reasonable to suggest that a unified set of intrusive processes is responsible for bringing younger material into this specific area.

The two dates >49 ^{14}C bp – which were never modeled because they are beyond the age of calibration – are also outliers. If such dates had appeared in the lower reaches of Lower T-Group, this would be consistent with expectations, but SWAP12-05 is in Upper T-Group, and SWAP12-02 is in S-Group. How did material >49 ^{14}C ka get incorporated into these contexts? Upward transport of charcoal via bioturbation or human activity from the undated lower reaches of Lower T-Group is unlikely, given that these layers yielded no charcoal despite intense recovery efforts. Just below this, PKT – BXA's basal stratum consisting of thick, hard volcanic deposits – is similarly bereft of charcoal. In the event that as-yet-undiscovered anthropic layers exist even farther below, transport across PKT is unrealistic. Given the improbability of local transport within the BXA, we must consider other parts of Mochena Borago as potential sources for this charcoal. Eastern parts of the rockshelter have strata >49 ka in age at higher elevations. It is possible that erosion or human activities may have caused the lateral transport of materials in a way that deposited old charcoal fragments from eastern Mochena Borago on a younger surface within the BXA. This is particularly likely for S-Group, where a paleofluvial channel has been observed. In light of this, Upper T-Group's substratum that yielded the other >49 ka date merits further examination.

The remaining five outliers differ from modeled age ranges by <5000 years (Supplementary data Table D). These smaller discrepancies might be due to formation processes and/or in-sample contamination. If sample contamination existed, more aggressive pretreatment could possibly have resolved the age difference. But this is purely speculative, as samples were too small for ABOx and/or pyrolysis pretreatments. Explanations that relate to formation processes must be considered so they can be evaluated during future fieldwork.

Two of the five (SWAP07-06 and SWAP08-05) are from lower portions of R-Group. These anomalously early dates are so similar and spatially proximate that they may be examined together (Table 2). Local bioturbation (transport up from S-Group within the BXA) is possible,

although we did not see any visual evidence of S-Group's more coarse-grained, pale, yellowish strata in this area. Another possibility – renewed lateral transport from eastern parts of the rockshelter – may be more probable, given that other observations point to standing water (which must have come from elsewhere), intermittent deposition and erosion episodes, and post-discard movement and damage to many R-Group lithics.

The remaining three outliers (SWAP08-03 in YBT, SWAP07-07 in S-Group, and SWAP14-12 in YBS) are each isolated cases in which a date is younger than expected and deviates from modeled age ranges by less than 5000 years. These could be accounted for either via individual contamination, or small-scale bioturbation events that might escape an excavator's notice.

6. Conclusion

Bayesian modeling, coupled with an enhanced array of radiocarbon dates, reshapes our view of the late Pleistocene chronology of the BXA within Mochena Borago Rockshelter in subtle but important ways. In some cases (e.g. YBT and YBS), the use of stratigraphic relationships to constrain the variability of dates has indeed generated more precise age ranges than the weighted mean model (cf. Bayliss and Bronk Ramsey, 2004). As excavation proceeds outside the BXA, having these "benchmark" strata may lend precision to sequences in other parts of the shelter. In other cases (S-Group), stratigraphic constraints provided more of the modeled information than the stratigraphic unit's individual dates themselves, all of which had low Agreement Index values (A < 60). This showcases another benefit of the Bayesian model: highlighting inconsistencies between modeled expectations and collected data. R-Group demonstrates the benefits of modeling age boundaries directly rather than estimating a single central tendency, as individual dates appear to cluster into two groups: six dates >40 ka and six <40 ka (Fig. 4).

Mochena Borago's significant number of outlier dates stems in part from Bayesian analysis' strict reliance on a stratigraphic model, such that residual or intrusive samples are highly likely to be identified as outliers. This positive development has practical consequences: either projects must become extremely selective in choosing dating samples (e.g., articulated faunal or human remains, structures, or other demonstrably intact features) whose contexts are so secure that the possibility of getting an outlier date is minimal (Bayliss, 2015:689), or projects must obtain a large number of dates (Douka et al., 2014) from reliable material (e.g., charcoal) that has been piece-plotted so as to allow iterative refinements in the stratigraphic model.

Research at Mochena Borago illustrates the benefits of the latter strategy. Finding outliers stimulates much-needed reflection about the contextual integrity of the Late Pleistocene assemblages from the BXA, and suggests complicated site formation processes that may involve multiple areas of the site. Rockshelters, including Ethiopian examples such as Porc-Épic (Assefa, 2006), are well-known for having complicated stratigraphy. Results presented here show the importance of painstaking methods applied over years of excavation and analysis (e.g., Marean, 2010). Only an exhaustive dating program could provide enough data points to distinguish between main depositional events and post-depositional processes. Individual piece plotting for all charcoal samples and most artifacts since 2007 will allow us to develop and implement criteria for separating primary vs. secondary contexts, and natural vs. cultural formation processes as we untangle the threads of Mochena Borago's complex depositional history.

Lithic technological data from Mochena Borago, now situated in a revised chronological framework, provide several insights into questions related to dispersals. The discovery of backed pieces in the deepest levels of Lower T-Group's undated sediments just above PKT suggests that this hafting strategy was practiced in SW Ethiopia closer to 60 ka rather than 50 ka, when hunter-gatherers began their early MIS 3 range expansion. It remains to be seen whether backing appeared even earlier in MIS 4, but as excavations outside the BXA penetrate recently discovered older strata (S. Brandt pers. obs.), Mochena Borago may help settle this question.

Obtaining precise ages for strata >50 ka will be challenging because of the impracticability of luminescence dating in areas exposed to volcanic activity. However, the planned establishment of a detailed tephrochronology for Mt. Damota and surrounding areas, combined with renewed attempts at argon dating, is one way to tackle this problem. Another is Obsidian Hydration Dating (OHD), which has not been used in Africa for decades because of reliability issues (Anovitz et al., 1999). New and refined methods of OHD are now being tested on obsidian artifacts from Mochena Borago specifically because of the site's well-dated sequence (C. Stevenson pers. comm.), which through the new age model has now been made even more secure.

One of the most striking aspects of Mochena Borago's cultural sequence is the longstanding maintenance of many core reduction strategies, including Levallois, right up to the stratigraphic hiatus beginning ~36 ka. Considering the rapid, dramatic climate oscillations of MIS 3, punctuated by major, possibly catastrophic volcanic events, such technological continuity is remarkable. It attests to strategies that were flexible enough to accommodate the unexpected. Indeed, for more than twenty millennia on Mt. Damota, "*plus ça change, plus c'est la même chose.*"

Supplementary data to this article can be found online at http://dx.doi.org/10.1016/j.jasrep.2016.09.013.

References

Aitken, M.J., 1990. Science-based Dating in Archaeology. Longman, London.

Anovitz, L.M., Elam, M., Riciputi, L., Cole, D., 1999. The failure of obsidian hydration dating: sources, implications, and new directions. J. Archaeol. Sci. 26, 735–752.

Armitage, S.J., Jasmin, S.A., Marks, A.E., Parker, A.G., Usik, V.I., Uerpmann, H.-P., 2011. The southern route "out of Africa": evidence for an early expansion of modern humans into Arabia. Science 331, 453–456.

Assefa, Z., 2006. Faunal remains from Porc-Epic: paleoecological and zooarchaeological investigations from a Middle Stone Age site in southeastern Ethiopia. J. Hum. Evol. 51, 50–75.

Bayliss, A., 2009. Rolling out revolution: using radiocarbon dating in archaeology. Radiocarbon 51 (1), 123–147.

Bayliss, A., 2015. Quality in Bayesian chronological models in archaeology. World Archaeol. 47 (4), 677–700.

Bayliss, A., Bronk Ramsey, C., 2004. Pragmatic Bayesians: a decade of integrating radiocarbon dates into chronological models. In: Buck, C.E., Millard, A. (Eds.), Tools for Constructing Chronologies: Crossing Disciplinary Boundaries. Springer, London, pp. 25–41.

Bayliss, A., Brock, F., Farid, S., Hodder, I., Southon, J., Taylor, R.E., 2015. Getting to the bottom of it all: a Bayesian approach to dating the start of Çatalhöyük. J. World Prehist. 28 (1), 1–26.

Benazzi, S., Douka, K., Fornai, C., Bauer, C., Kullmer, O., Svoboda, J., Pap, I., Mallengi, F., Bayle, P., Coquerelle, M., Condemi, S., Ronchitelli, A., Harvati, K., Weber, G., 2011.

Early dispersal of modern humans in Europe and implications for Neanderthal behaviour. Nature 479, 525–528.

Bermensolo, 2013. K., Flaked Stone Artifacts From the R-Group at the Mochena Borago Rockshelter, Ethiopia, and Their Implications. Unpublished M.A. qualifying paper on file,. University of Florida, Gainesville.

Bird, M.I., Ayliffe, L.K., Fifield, L.K., Turney, C.S.M., Cresswell, R.G., Barrows, T.T., David, B., 1999. Radiocarbon dating of "old" charcoal using a wet oxidation, stepped-combustion procedure. Radiocarbon 41 (2), 127–140.

Brandt, S.A., 1986. The upper Pleistocene and early Holocene prehistory of the Horn of Africa. Afr. Archaeol. Rev. 4, 41–82.

Brandt, S.A., Brook, G.A., 1984. Archaeological and paleoenvironmental research in northern Somalia. Curr. Anthropol. 25 (1), 119–121.

Brandt, S.A., Gresham, T.H., 1989. L'age de la pierre en Somalie. l'Anthropologie 94 (3), 459–482.

Brandt, S., Weedman, K., 2002. Woman the toolmaker. Archaeology 55 (5), 50–53.

Brandt, S.A., Fisher, E.C., Hildebrand, E.A., Vogelsang, R., Ambrose, S.H., Lesur, J., Wang, H., 2012. Early MIS 3 occupation of Mochena Borago rockshelter, southwest Ethiopian highlands: implications for Late Pleistocene archaeology, paleoenvironments and modern human dispersals. Quat. Int. 274, 38–54.

Brock, F., Higham, T., Ditchfield, P., Bronk Ramsey, C., 2010. Current pre-treatment methods for AMS radiocarbon dating at the Oxford Radiocarbon Accelerator Unit (ORAU). Radiocarbon 52, 103–112.

Bronk Ramsey, C., 2001. Development of the radiocarbon calibration program OxCal. Radiocarbon 43, 355–363.

Bronk Ramsey, C., 2009a. Bayesian analysis of radiocarbon dates. Radiocarbon 51, 337–360.

Bronk Ramsey, C., 2009b. Dealing with outliers and offsets in radiocarbon dating. Radiocarbon 51 (3), 1023–1045.

Buck, C.E., Cavanagh, W.G., Litton, C.D., 1996. Bayesian Approach to Interpreting Archaeological Data. John Wiley & Sons, West Sussex.

Clark, J.D., Williamson, K.D., 1984. A Middle Stone Age occupation site at Porc Epic cave, Dire Dawa (east-central Ethiopia), part I. Afr. Archaeol. Rev. 2, 37–64.

Diez-Martín, F., Domínguez-Rodrigo, M., Sánchez, P., Mabulla, A.Z.P., Tarriño, R.B., Prendergast, M.E., de Luque, L., 2009. The Middle to Later Stone Age technological transition in East Africa. New data from Mumba rockshelter Bed V (Tanzania) and their implications for the origin of modern human behavior. J. Afr. Archaeol. 7, 147–173.

Douka, K., Jacobs, Z., Lane, C., Grün, R., Farr, L., Hunt, C., Inglis, R., Reynolds, T., Albert, P., Aubert, M., Cullen, V., Hill, E., Kinsley, L., Roberts, R., Tomlinson, E., Wulf, S., Barker, G., 2014. The chronostratigraphy of the Haua Fteah cave (Cyrenaical northeast Libya). J. Hum. Evol. 66, 39–63.

Drake, N., Breeze, P., 2016. Climate change and modern human occupation of the Sahara from MIS 6-2. In: Jones, S.C., Stewart, B.A. (Eds.), Africa from MIS 6-2: Population Dynamics and Paleoenvironments. Springer, Dordrecht, pp. 103–122.

Drake, N.A., Breeze, P., Parker, A., 2013. Palaeoclimate in the Saharan and Arabian deserts during the Middle Palaeolithic and the potential for hominin dispersals. Quat. Int. 300, 48–61.

Fisher, E., 2010. Late Pleistocene Technological Change and Hunter-Gatherer Behavior at Moche Borago Rockshelter, Sodo-Wolayta, Ethiopia: Flaked Stone Artifacts From the Early OIS 3 (60–43 ka) Deposits. Unpublished PhD dissertation,. University of Florida, Gainesville.

Galbraith, R.F., Roberts, R.G., Laslett, G.M., Yoshida, H., Olley, J.M., 1999. Optical dating of single and multiple grains of quartz from Jinmium rock shelter, northern Australia, part I: experimental design and statistical models. Archaeometry 41, 339–364.

Galbraith, R.F., Roberts, R.G., Yoshida, H., 2005. Error variation in OSL palaeodose estimates from single aliquots of quartz: a factorial experiment. Radiat. Meas. 39, 289–307.

Gliganic, L.A.G., 2011. Optically and Infrared Stimulated Luminescence Investigations of the Middle and Later Stone Age in East Africa. Unpublished PhD dissertation,. University of Wollongong, Wollongong/Australia.

Goder-Goldberger, M., 2013. The Khormusan: evidence for an MSA east African industry in Nubia. Quat. Int. 300, 182–194.

Gresham, T.H., 1984. An Investigation of an Upper Pleistocene Archaeological Site in Northern Somalia. Unpublished M.A. thesis,. University of Georgia.

Gutherz, X., 2000. Sondages dans l'abri sous-roche de Moche Borago Gongolo dans le Wolayta (Ethiopie). Annales d'Ethiopie XVI 35–38.

Gutherz, X., Jallot, L., Lesur, J., Pouzolles, G., Sordoillet, D., 2002. Les fouilles de l'abri sous-roche de Moche Borago (Soddo, Wolyata). Premier bilan. Annales d'Ethiopie XVIII 181–190.

Gutherz, X., Diaz, A., Ménard, C., Bon, F., Douze, K., Léa, V., Lesur, J., Sordoillet, D., 2014. The Hargeisan revisited: lithic industries from shelter 7 of Laas Geel, Somaliland and the transition between the Middle and Late Stone Age in the Horn of Africa. Quat. Int. 343, 69–84.

Haesaerts, P., Damblon, F., Nigst, P., Hublin, J.-J., 2013. ABA and ABOx radiocarbon cross-dating on charcoal from middle Pleniglacial loess deposits in Austria, Moravia, and western Ukraine. Radiocarbon 55 (2–3), 641–647.

Henn, B.M., Botigué, L.R., Gravel, S., Wang, W., Brisbin, A., Byrnes, J.K., Fadhlaoui-Zid, K., Zalloua, P., Moreno-Estrada, A., Bertranpetit, J., Bustamante, C.D., Comas, D., 2012. Genomic ancestry of north Africans supports back-to-Africa migrations. PLoS Genet. 8, e1002397.

Higham, T., Ramsey, C.B., Karavanic, I., Smith, F.H., Trinkaus, E., 2006. Revised direct radiocarbon dating of the Vindija G1 Upper Paleolithic Neanderthals. Proc. Natl. Acad. Sci. U.S.A. 103 (3):553–557. http://dx.doi.org/10.1073/pnas.0510005103.

Higham, T., Brock, F., Peresani, M., Broglio, A., Wood, R., Douka, K., 2009. Problems with radiocarbon dating the middle to upper Palaeolithic transition in Italy. Quat. Sci. Rev. 28, 1257–1267.

Higham, T., Compton, T., Stringer, C., Jacobi, R., Shapiro, B., Trinkaus, E., Chandler, B., Gröning, F., Collins, C., Hillson, S., O'Higgins, P., FitzGerald, P., Fagan, M., 2011. The earliest evidence for anatomically modern humans in northwestern Europe. Nature 479, 521–524.

Hiscock, P., 2015. Making it small in the Palaeolithic: bipolar stone-working, miniature artifacts, and models of core recycling. World Archaeol. 47 (1), 158–169.

Hovers, E., 2006. Neanderthals and modern humans in the Middle Paleolithic of the Levant: what kind of interaction? In: Conard, N. (Ed.), When Neanderthals and Modern Humans Met. Kerns Verlag, Tubingen, pp. 65–86

Hughen, K., Southon, J., Lehman, S., Bertrand, C., Turnbull, J., 2006. Marine-derived ^{14}C calibration and activity record for the past 50,000 years updated from Cariaco Basin. Quat. Sci. Rev. 25, 3216–3227.

Jones, S., Antoniadou, A., Barton, H., Drake, N., Farr, L., Hunt, C., Inglis, R., Reynolds, T., White, K., Barker, G., 2016. Patterns of hominin occupation and cultural diversity across the Gebel Akhdar of northern Libya over the last ~200 kyr. In: Jones, S.C., Stewart, B.A. (Eds.), Africa From MIS 6-2: Population Dynamics and Paleoenvironments. Springer, Dordrecht, pp. 77–122.

Karkanas, P., Brown, K.S., Fisher, E., Jacobs, Z., Marean, C.W., 2015. Interpreting human behavior from depositional rates and combustion features through the study of sedimentary microfacies at site Pinnacle Point 5–6, South Africa. J. Hum. Evol. 85, 1–21.

Klein, R., 2009. The Human Career. 3rd Edition. University of Chicago Press, Chicago.

Knicker, H., Müller, P., Hilscher, A., 2007. How useful is chemical oxidation with dichromate for the determination of "black carbon" in fire-affected soils? Geoderma 142, 178–196.

Leplongeon, A., 2014. Microliths in the Middle and Later Stone Age of eastern Africa: new data from Porc-Epic and Goda Buticha cave sites, Ethiopia. Quat. Int. 343, 100–116.

Leplongeon, A., Pleurdeau, D., 2011. The Upper Paleolithic lithic industry of Nazlet Khater 4 (Egypt): implications for the Stone Age/Palaeolithic of northeastern Africa. Afr. Archaeol. Rev. 28, 213–236.

Marean, C.W., 2010. Introduction to the special issue: the Middle Stone Age at Pinnacle Point site 13B, a coastal cave near Mossel Bay (Western Cape province, South Africa). J. Hum. Evol. 59, 231–233.

Marks, A., 1968. The Khormusan: an upper Pleistocene industry in Sudanese Nubia. In: Wendorf, F. (Ed.), The Prehistory of Nubia Vol. 1. Fort Burgwin Research Center and Southern Methodist University Press, Dallas, pp. 315–391.

McBrearty, S., Brooks, A., 2000. The revolution that wasn't: a new interpretation of the origins of modern behavior. J. Hum. Evol. 39 (5), 453–563.

Mellars, P., 2006. Going east: new genetic and archaeological perspectives on the modern human colonization of Eurasia. Science 313, 796–800.

Mellars, P., Gori, K.C., Carr, M., Soares, P.A., Richards, M.B., 2013. Genetic and archaeological perspectives on the initial modern human colonization of southern Asia. PNAS 110 (26), 10699–10704.

Ménard, C., 2015. Ruptures et continuités dans le Late Stone Age de la Corne de l'Afrique: apports des industries lithiques du Rift éthiopien. PhD dissertation,. Université Toulouse–Jean Jaurès.

Ménard, C., Bon, F., Dessie, A., Bruxelles, L., Douze, K., Fauvelle, F.-X., Khalidi, L., Lesur, J., Mensan, R., 2014. Late Stone Age variability in the main Ethiopian rift: new data from the Bulbula River, Ziway-Shala Basin. Quat. Int. 343, 53–68.

Mercier, N., Valladas, H., Froget, L., Joron, J.-L., Vermeersch, P.M., Van Peer, P., Moeyersons, J., 1999. Thermoluminescence dating of a middle Palaeolithic occupation at Sodmein Cave, Red Sea mountains (Egypt). J. Archaeol. Sci. 26, 1339–1345.

Meyer, S., Bödeker, O., Fisher, E., Kehl, M., Brandt, S., Goldberg, P., Vogelsang, R., Zinaye, B., Bubenzer, O. in prep. Deciphering Rockshelter Evolution and Sediment Deposition in Volcanic, Mountainous, Tropical Humid Landscapes: The Case of Mochena Borago (Ethiopian Highlands). (Submitted in May 2016 to Geoarchaeology – An International Journal).

Moeyersons, J., Vermeersch, P.M., Van Peer, P., 2002. Dry cave deposits and their palaeoenvironmental significance during the last 115 ka, Sodmein Cave, Red Sea mountains, Egypt. Quat. Sci. Rev. 21, 837–851.

Müller, U.C., Pross, J., Tzedakis, P.C., Gamble, C., Kotthoff, U., Schmiedl, G., Wulf, S., Christanis, K., 2011. The role of climate in the spread of modern humans into Europe. Quat. Sci. Rev. 30, 273–279.

Parow-Souchon, H., 2013. Die Klingentechnologie von Mochena Borago/Äthiopien. Innovation vor 40.000 Jahren. Master's thesis,. University of Cologne.

Parow-Souchon, H., Vogelsang, R., Brandt, S.A. n.d. Blade Production at Mochena Borago Rockshelter, Ethiopia: A Contribution to MIS 3 Technological Variability in the Horn of Africa. (Manuscript in preparation).

Parton, A., Farrant, A.R., Leng, M.J., Schwenninger, J.-L, Rose, J.I., Uerpmann, H.-P., Parker, A.G., 2013. An early MIS 3 pluvial phase in southeast Arabia: climatic and archaeological implications. Quat. Int. 300, 62–74.

Pleurdeau, D., 2005. Human technical behavior in the African Middle Stone Age: the lithic assemblage of Porc-Epic cave (Dire Dawa, Ethiopia). Afr. Archaeol. Rev. 22, 177–197.

Pleurdeau, D., Hovers, E., Assefa, Z., Asrat, A., Pearson, O.M., Bahain, J.-J., Lam, Y.M., 2014. After the dispersal: cultural change or continuity in the late MSA/early LSA of southeastern Ethiopia? The site of Goda Buticha, Dire Dawa area. Quat. Int. 343, 117–135.

Rebollo, N.R., Weiner, S., Brock, F., Meignen, L., Goldberg, P., Belfer-Cohen, A., Bar-Yosef, O., Boaretto, E., 2011. New radiocarbon dating of the transition from the middle to upper Paleolithic in Kebara Cave, Israel. J. Archaeol. Sci. 38, 2424–2433.

Reimer, P.J., Bard, E., Bayliss, A., Beck, J.W., Blackwell, P.G., Bronk Ramsey, C., Buck, C.E., Cheng, H., Edwards, R.L., Friedrich, M., Grootes, P.M., Guilderson, T.P., Haflidason, H., Hajdas, I., Hatté, C., Heaton, T.J., Hoffmann, D.L., Hogg, A.G., Hughen, K.A., Kaiser, K.F., Kromer, B., Manning, S.W., Niu, M., Reimer, R.W., Richards, D.A., Scott, E.M., Southon, J.R., Staff, R.A., Turney, C.S.M., van der Plicht, J., 2013. IntCal13 and Marine13 radiocarbon age calibration curves 0–50,000 years cal BP. Radiocarbon 55 (4), 1869–1887.

Rethemeyer, J., Fülöp, R.-H., Höfle, S., Wacker, L., Heinze, S., Hajdas, I., Patt, U., König, S., Stapper, B., Dewald, A., 2013. Status report on sample preparation facilities for ^{14}C analysis at the new Cologne AMS center. Nucl. Inst. Methods Phys. Res. B 294, 168–172.

Rosso, D.E., d' Errico, F., Zilhão, J., 2014. Stratigraphic and spatial distribution of ochre and ochre processing tools at Porc-Epic Cave, Dire Dawa, Ethiopia. Quat. Int. 343, 85–99.

Santos, G.M., Bird, M.I., Parenti, F., Fifield, L.K., Guidon, N., Hausladen, P.A., 2003. The controversial antiquity of the peopling of the Americas: a review of the chronology of the lowest occupation layer in the Pedra Furada rock shelter, Piauí, Brazil. Quat. Sci. Rev. 22, 2303–2310.

Schmidt, C., Kindermann, K., Van Peer, P., Bubenzer, O., 2015. Multi-emission luminescence dating of heated chert from the Middle Stone Age sequence at Sodmein Cave (Red Sea mountains, Egypt). J. Archaeol. Sci. 63, 94–103.

Sellet, F., 1995. Levallois or not Levallois: does it really matter? Learning from an African case. In: Dibble, H.L., Bar-Yosef, O. (Eds.), The Definition and Interpretation of Levallois TechnologyMonographs in World Archaeology No. 23. Prehistory Press, Madison Wisconsin, pp. 25–39.

Shea, J.J., 2008. Transitions or turnovers? Climatically-forced extinctions of *Homo sapiens* and Neandertals in the east Mediterranean Levant. Quat. Sci. Rev. 27, 2253–2270.

Soares, P., Alshamali, F., Pereira, J., Fernandes, V., Silva, N.M., Alfonso, C., Costa, M., Misilova, E., Macaulay, V., Richards, M., Cerny, V., Pereira, L., 2011. The expansion of mtDNA Haplogroup L3 within and out of Africa. Mol. Biol. Evol. http://dx.doi.org/10.1093/molbev/msr245.

Soares, P., Rito, T., Pereira, L., Richards, M.B., 2016. A genetic perspective on African prehistory. In: Jones, S.C., Stewart, B.A. (Eds.), Africa from MIS 6-2: Population Dynamics and Paleoenvironments. Springer, Dordrecht, pp. 383–405.

Stewart, B.A., Jones, S.C., 2016. Africa from MIS 6-2: the fluorescence of modern humans. In: Jones, S.C., Stewart, B.A. (Eds.), Africa from MIS 6-2: Population Dynamics and Paleoenvironments. Springer, Dordrecht, pp. 1–22.

Stewart, J.R., Stringer, C.B., 2012. Human evolution out of Africa: the role of refugia and climate change. Science 335, 1317–1321.

Stokes, S., Bailey, R., 2002. Optical dating of Nazlet Safaha and Nazlet Khater. In: Vermeersch, P. (Ed.), Palaeolithic Quarrying Sites in Upper and Middle Egypt. Leuven University Press, Leuven, pp. 349–350.

Stuiver, M., Polach, H., 1977. Reporting of 14C data. Radiocarbon 19, 355–363.

Suess, H.E., 1967. Bristlecone pine calibration of the radiocarbon time scale from 4100 BC to 1500 BC. In: staff, I.A.E.A. (Ed.), Radioactive Dating and Low-Level Counting: Proceedings of a Symposium Organized by the International Atomic Energy Agency (IAEA) in Cooperation With the Joint Commission on Applied Radioactivity (ICSU). International Atomic Energy Agency (IAEA), Vienna, pp. 143–152 Monaco, 2–10 March 1967.

Taylor, R.E., Bar-Yosef, O., 2014. Radiocarbon Dating: An Archaeological Perspective. 2nd Edition. Left Coast Press, Walnut Creek.

Turney, C.S.M., Bird, M.I., Fifield, L.K., Roberts, R.G., Smith, M.A., Dortch, C.E., Grün, R., Lawson, E., Ayliffe, L.K., Miller, G.H., Dortch, J., Cresswell, R.G., 2001. Early human occupation at Devil's Lair, southwestern Australia 50,000 years ago. Quat. Res. 55, 3–13.

Van Peer, P., 1991. New observations about the Nile Valley middle Palaeolithic: Safaha method and lateralization of Levallois flakes. Paléorient 17 (2), 135–142.

Van Peer, P., 2016. Technological systems, population dynamics, and historical process in the MSA of Northern Africa. In: Jones, S.C., Stewart, B.A. (Eds.), Africa from MIS 6-2: Population Dynamics and Paleoenvironments. Springer, Dordrecht, pp. 147–160.

Van Peer, P., Vermeersch, P.M., 2000. The Nubian complex and the dispersal of modern humans in north Africa. In: Krzyzaniak, L., Kroeper, K. (Eds.), Recent Research into the Stone Age of Northeastern Africa. Studies in African Archaeology 7, pp. 47–60 Poznan Archaeological Museum.

Van Peer, P., Vermeersch, P.M., Moeyersons, J., 1996. Palaeolithic stratigraphy of Sodmein Cave (Red Sea mountains, Egypt). Seminar on geo-archaeology in tropical and Mediterranean regions. Royal Academy of Overseas Sciences, Brussels. Geo-Eco-Trop. 20 (1–4), 61–71.

Van Peer, P., Vermeersch, R.M., Paulissen, E., 2010. Chert quarrying, lithic technology and a modern human burial at the Palaeolithic site of Taramsa 1, upper Egypt. Egyptian Prehistory Monographs. Leuven University Press, Leuven.

Vermeersch, P.M., 2002. Geomorphology of the Nazlet Khater area. In: Vermeersch, P. (Ed.), Palaeolithic Quarrying Sites in Upper and Middle Egypt. Leuven University Press, Leuven, pp. 21–25.

Vermeersch, P.M., Paulissen, E., Vanderbeken, T., 2002. Nazlet Khater 4: an upper Palaeolithic underground chert mine. In: Vermeersch, P. (Ed.), Palaeolithic Quarrying Sites in Upper and Middle Egypt. Leuven University Press, Leuven, pp. 211–271.

Wang, H., Hackley, K.C., Panno, S.V., Coleman, D.D., Liu, J.C.-L., Brown, J., 2003. Pyrolysis combustion ^{14}C dating of soil organic matter. Quat. Res. 60, 348–355.

Wang, H., Ambrose, S.H., Hedman, K.M., Emerson, T.E., 2010. AMS ^{14}C dating of human bones using sequential pyrolysis and combustion of collagen. Radiocarbon 52, 157–163.

Warren, A., 2010. Preliminary Characterization and Provenance of Obsidian Artifacts From Ethiopian Archaeological Sites Using Portable X-ray Fluorescence. Unpublished BA thesis,. University of Florida, Gainesville.

Wendorf, F., Schild, R., Herbert, H., 1979. A new radiocarbon chronology for prehistoric sites in Nubia. J. Field Archaeol. 6 (2), 219–223.

Weninger, B., Jöris, O., 2008. A ^{14}C age calibration curve for the last 60 ka: the Greenland-Hulu U/Th timescale and its impact on understanding the middle to upper Paleolithic transition in western Eurasia. J. Hum. Evol. 55, 772–781.

Whittle, A., Bayliss, A., Healy, F., 2008. The timing and tempo of change: examples from the fourth millennium cal. BC in southern England. Camb. Archaeol. J. 18 (1):65–70. http://dx.doi.org/10.1017/S0959774308000061.

Wurz, S., Van Peer, P., 2012. Out of Africa, the Nile Valley and the northern route. S. Afr. Archaeol. Bull. 67 (196), 168–179.